UCRL-JC-131330
Preprint

ARAC Simulation of the Algeciras, Spain Steel Mill CS-137 Release

P. J. Vogt, B. M. Pobanz, F. J. Aluzzi, R. L. Baskett and T. J. Sullivan

This paper was prepared for submittal to
American Nuclear Society 1998 Winter Meeting
Washington, DC
November 15-19, 1998

February 1, 1999

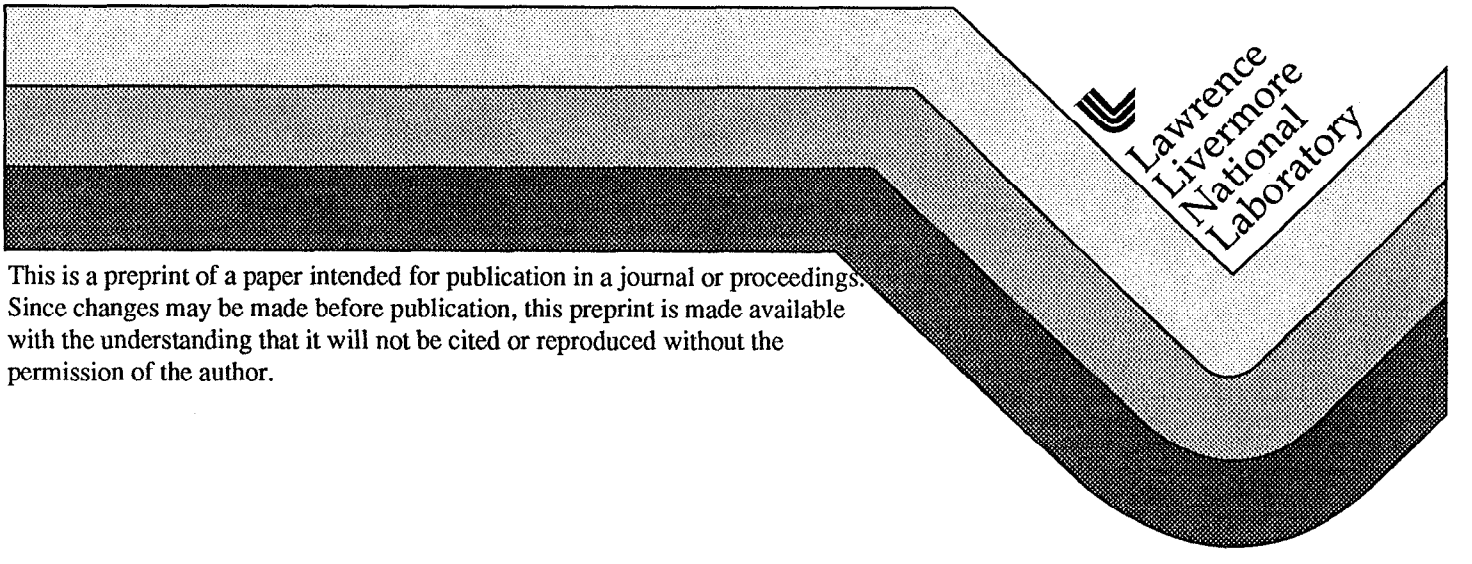

DRAFT

ARAC SIMULATION OF THE ALGECIRAS, SPAIN STEEL MILL CS-137 RELEASE

by

Philip J. Vogt
Brenda M. Pobanz
Fernando J. Aluzzi
Ronald L. Baskett
Thomas J. Sullivan

September 1998

Atmospheric Release Advisory Capability
Lawrence Livermore National Laboratory
Livermore, California

DRAFT

2/3/99

TABLE OF CONTENTS

FIGURES

ARAC SIMULATION OF THE ALGECIRAS, SPAIN STEEL MILL CS-137 RELEASE

ABSTRACT

On 12 June 1998, the Atmospheric Release Advisory Capability (ARAC) learned from news reports about the accidental release of cesium-137 from a steel mill near Algeciras, Spain. This paper presents a series of three calculations we made as we learned more about the incident. Initially we only knew that a Cs-137 release occurred near Algeciras. Details about the location, date and time, and amount of the release were not available. The ARAC program leader contacted European colleagues, who responded with preliminary set of ambient cesium air concentration data. In the weeks that followed we made three sets of dispersion model calculations, each with somewhat different initial conditions. This report summarizes our calculations and demonstrates our ability to derive a source term from a limited set of concentration measurements.

We used the U.S. Navy Operational Global Atmospheric Prediction System (NOGAPS) gridded data for meteorological input into our diagnostic models. To better resolve near-release location and coastal meteorological conditions, for the third set we blended four days of WMO surface and upper air observations with the gridded data.

Our calculations showed the plume initially traveled eastward over the Mediterranean Sea, turned northward into France, Italy, and Switzerland, and was split by the Alps. For each calculation we determined the timing and amount of cesium released by fitting our modeled air concentrations to the available set of measurements. A small set of ratios of the measured to computed air concentrations paired in space and time showed that our results produced similar statistics to those achieved in previous more extensive ARAC model evaluation studies on the continental scale.

Fortunately the release was too small to produce any plausible health effects, but the incident elucidates the point that accidents involving even small quantities of hazardous materials can be detected over large regions. This case study serves as a reminder that large accidental releases have the potential to impact substantial geographic areas and populations.

INTRODUCTION

ARAC Program

ARAC is a real-time emergency response organization that evaluates effects from releases of hazardous material to the atmosphere (Sullivan *et. al.* 1993). Located at University of California's Lawrence Livermore National Laboratory, ARAC's primary function is to support the Department of Energy (DOE) and Department of Defense (DoD) for radiological releases. ARAC has also assisted several other federal, state and local agencies. Since 1979, ARAC has responded to more than 100 alerts, accidents, and disasters, and supported more than 1000 exercises. Besides accidental radiological releases, ARAC has assessed natural disasters such as volcanic ash cloud, manmade disasters such as the Kuwaiti oil fires, and several chemical accidents.

ARAC Emergency Response Modeling System

ARAC's Emergency Response Operating System employs a series of five codes to model any size problem anywhere in the world (ARAC 1996). Figure 1 illustrates the modeling steps. To develop the underlying topographic setting, ARAC maintains a terrain database at 500 m resolution with nearly global coverage. The first of the five codes, TOPOG, converts the terrain data to a block-cell representation of the model domain.

ARAC obtains real-time worldwide observed meteorological data from the Air Force Weather Agency, and gridded data provided by global operational forecast models of the U.S. Navy and NOAA. These data are interpolated by the second code, the diagnostic Meteorological Data Interpolation Code (MEDIC) to create a series of 3-D wind arrays. Based on the terrain and regional atmospheric stability, the third code, MATHEW, creates a mass-adjusted wind field from the interpolated MEDIC gridded winds, observed data, or a combination of both. The fourth code, ADPIC, a Lagrangian Random Displacement Model, simulates the dispersion of the released material with thousands of marker particles. The code advects and disperses the material, keeping track of the modeled concentration at grid points or specified locations in the domain.

The fifth code, PLOT CONTOUR, converts the ADPIC marker particle densities to contours of interest such as doses for radiological accidents, air concentrations for chemical releases, or ground deposition. Contours are displayed on a map of the model domain generated from geographical map databases. An optional sixth code, TIME HISTORY, compares calculated values with observed measurements at specified times and locations.

Notification of the Accident

On 9 June 1998, the Swiss government announced that radiation levels up to 1000 times background had been detected in their national monitoring network and that the source was unknown; France and Italy reported similar measurements. On the next day a steel mill near Algeciras, located near the extreme southern tip of Spain (Fig. 2), notified the Spanish Nuclear Security Agency (CSN) that they had detected radiation in one of their oven filtration systems. On 12 June the Spanish government revealed that a medical radiotherapy source of Cs-137 was apparently melted in the Acerinox steel mill scrap metal furnace and subsequently released into the atmosphere. However, the CSN did not observe elevated radiation levels in their network. The amount and the time of the release were

unknown, but the incident was thought to have taken place during the last week of May 1998. On 12 June the International Atomic Energy Agency (IAEA) Emergency Response Centre issued a bulletin announcing the occurrence of the radiological incident, and the possible connection to elevated levels of Cs-137 detected at the end of May and early June in southern Europe.

ARAC became aware of the incident when news services reported the accident on 12 June in the United States. These news stories indicated that elevated levels of Cs-137 had been detected in France and Switzerland, and in a related update bulletin, that the steel-mill near Algeciras was the suspected source. We began by accessing our archived gridded meteorological data from the area, but did not begin modeling the incident until we received measurement data from several countries.

Measurement Data and ARAC Simulations

In response to inquiry by the ARAC program on 13-15 June, colleagues in Spain, France, Switzerland, Italy, Sweden, and the European Union provided us with Cs-137 air concentration measurements for 25 May - 8 June. Figure 3 shows sampler locations and Appendix 1 lists names and locations of the measurements we received. We made the first model run after we received the initial set of measurements. In the three weeks that followed, as we received more measurements and corrected measurement data, we made two additional sets of calculations. Table 1 summarizes the key input information for each of the three sets of calculations.

Table 1. Summary of ARAC simulations for the Algeciras release

ARAC Set No.	Date Set Released	Source Location	Release Time, Duration	Release Amount	Model Grid	No. of Meas.	Meteorological Data
1	18 June 1998	5°22' 53"W 36° 11' 15"N ARAC estimate	29 May 1998 0900 UTC, 12 hr	110 Ci	1800 x 1800 km	22	1° NOGAPS gridded data
2	26 June 1998	Same as Set 1	29 May 1998 1500 UTC, 30 min	50 Ci	2600 x 2600 km	58	1° NOGAPS gridded data
3	9 July 1998	5° 26' W 36° 10' N Spanish Govt.	30 May 1998 0130 UTC, 30 min	50 Ci	Same as Set 2	117	1° NOGAPS gridded data with first 4 days observations

Appendix 2 lists the above-detection threshold measurement data and our results for each of the three sets. Various countries made Cs-137 air concentration measurements with different samplers, averaging times (from one to 14 days), and radiological sensitivities (thresholds), so the quality of the data may vary. We assumed that all measurements were obtained near the ground at a height of 1.5 m. With the exception of data provided from Ispra and two measurements in France, precise start or end times were not provided with the measurements. We prescribed start and stop times of 1200 UTC for all data. (For example we assumed that a measurement from 1 June to 3 June was valid from 1200 UTC 1 June to 1200 UTC 3 June.) This allowed close comparison to the 1100 UTC start/stop times for the Ispra data.

Synoptic Weather Pattern

The release occurred during a fairly weak and persistent summertime weather pattern. Figure 4 shows 1200 UTC analysis fields for the ECMWF obtained from archive of 500 hPa heights and surface pressure contours. Figure 4a, valid on 30 May 1990, shows a cut-off area of low heights extending from the Bay of Biscay eastward over the Atlantic. Surface pressure contours on the same figure show two areas of low pressure associated with this upper-air system, one located near Brittany, and a deeper low southwest of Ireland. Winds aloft and at the surface appear to be westerly over Gibraltar Strait and southern Spain.

Figures 4b-d, valid on 1200 UTC on 31 May, 01 and 02 June, show the synoptic pattern coinciding with the start of the release and the period of plume transport over the western Mediterranean Sea. The cut-off area of low heights at 500 hPa begins to slowly open up over the next three days as heights fall over western Scandinavia associated with a stronger upper-air feature. The position and axis of the trough remains fairly stationary during this period, staying west of the Iberian Peninsula and France.

Mostly westerly flow prevails over Spain on 30 May at 1200 UTC (Figure 4b), becoming southwesterly by 1200 UTC on 01 June (Figure 4c), and with height rises over the Pyrennes and France. Flow aloft becomes more southerly over Spain and the western Mediterranean Sea by 1200 UTC on 02 June (Figure 4d).

At the surface, the weak low near Brittany on the 30th moved over southern Norway (Figure 4b), while a new surface low is approaching the western edge of the analysis (evident by the troughing west of Portugal). By 1200 UTC on 01 June (Figure 4c) the trough moved around the quasi-stationary, anchor low and is located over the Bay of Biscay. Surface winds over Spain and the western Mediterranean appear to become more southwesterly from westerly, with more relaxed contour gradients over the Mediterranean. At 1200 UTC on 02 June a surface low developed from the trough and continued to move around the anchor low to southern England (Figure 4d).

As we did not process any synoptic precipitation data for Europe, we did not apply wet deposition in our calculations.

SET 1 (INITIAL) SIMULATION

Model Grid

We selected a model domain extending 1800 km in the horizontal and 3000 m in the vertical. This grid maximized the terrain resolution while encompassing the suspected release area and the highest air concentration measurements in southern Europe (Fig. 5). We used 80 x 80 horizontal cells with 30 vertical layers, resulting in 22.5 km horizontal and 100 m (constant) vertical resolution (Fig. 6).

Meteorological Data

We used the U.S. Navy Operational Global Atmospheric Prediction System (NOGAPS) gridded data with one-degree resolution. We used analysis fields for each day at 0000 and 1200 UTC, as well as the 6-hr forecast valid at 0600 and 1800 UTC from the

associated 0000 UTC or 1200 UTC model run. We generated wind fields every 6 hr centered on the NOGAPS data time, i.e., we used the 1200 UTC NOGAPS winds from 0900 through 1500 UTC. Additionally, we linearly interpolated wind fields between meteorological data sets.

Figure 7a shows that the modeled surface winds flowed from the west over Gibraltar Strait and turned to the north near the Balearic Islands at 0300 UTC on 30 May. Surface winds were weaker, but generally southwesterly over the western Mediterranean at 0300 UTC on 31 May (Fig. 7b). They became light, southerly and easterly flows at 0300 UTC on 1 June (Fig. 7c). By 0300 UTC on 2 June (Fig. 7d) an anticyclonic flow developed over the area.

Figure 8a shows that model winds at 1500 m (one-half depth of model) at 0300 UTC on 30 May (Fig. 8a) are similar to the surface winds. By 0300 UTC on 31 May (Fig. 8b), the closed low near Brittany has opened up into a broad trough with strong southwesterly flow extending to Sardinia and Corsica. An upper air disturbance moving through the trough generated stronger southwesterly flow over Portugal and Spain by 0300 UTC on 1 June (Fig. 8c), and at 0300 UTC on 2 June southwesterly flow prevailed over much of the grid except south of the Alps where westerly flow occurred (Fig. 8d).

Dispersion Parameters

For the initial calculations we used a diurnally-varying boundary layer depth. We defined four 6-hr periods – day, night, and two transitions. As we did not have observational soundings for the initial set, we used our judgment to determine appropriate boundary layer heights and atmospheric stability. For the first two days when the plume was over water, we initially fixed the boundary layer height at 500 m. Beginning on the third day, we used 350 m at night, 1250 m during the day, and 500 m for the transitional periods was used. Due to the scale of the calculation, we fixed the atmospheric stability at neutral and used our long-range horizontal dispersion parameterization throughout the calculations.

Source Term Assumptions

As we initially did not know the release coordinates, we assumed the release came from one of two 183 m high stacks located on a DoD Operational Navigational Chart just north of Gibraltar. We assumed the buoyant release produced 100 m plume rise above the stack. Additionally, since release amount and time were not available, we used a normalized source rate of 1 Ci/s and a series of 3-hr puffs released every 6 hr beginning on 27 May and ending on 31 May. We assumed the Cs-137 released from the stack was a combustion-product particulate with a 0.5 μm median diameter and had a log-normal particle size distribution ranging from 0.1-1.0 μm.

Results

We compared our model results from each of the 3-hr puffs separately to the highest average air concentration measurements. We selected measurements greater than 100 $\mu Bq/m^3$ because of the uncertainty associated with low concentrations. Once we found a puff release period which best matched the timing, we made additional model iterations to refine the source term amount. After six additional iterations, the comparison of the normalized model-calculated source to the measurements indicated slightly more than 100

Ci of Cs-137 was likely to have been released over a 12-hr period beginning at 0900 UTC (0700 local) on 29 May ending at 2100 UTC (1900 local) the same day.

Figure 9 shows averaged air concentrations near the ground for Set 1. Figure 9a shows the one-day air concentration ending at 0900 UTC on 30 May. The plume shows the largest latitudinal extent due to the 12-hr release and variations in horizontal wind direction over that period. By 0900 UTC on 31 May (Fig. 9b), the plume extends over the western Mediterranean, with the plume edge extending from the coast of Spain to the coast of Algeria, and extensively covers the Balearic Islands. Figure 9c shows that the plume just reached the coasts of Italy and France by 0900 UTC on 1 June, and extends into central France and off the eastern edge of the domain by 0900 UTC on 2 June (Fig. 9d). The highest concentrations are over southern France (the French Riviera), with much of the plume turning northward, west of the Alps, and a portion moving eastward south of the Alps over Italy.

Figure 10 shows the average air concentration for the first 5 days. The axis of the plume remains entirely over the Mediterranean Sea, passing over the Balearic Islands.

As stated above, we selected only the measurements greater than 100 $\mu Bq/m^3$ to determine the source amount. Appendix 2 shows that the model compares well with the highest values at Toulon, Nice, Cadarache, and Monte Ceneri (each within a factor of two) and worse at Montpellier (within a factor of 5). We used the original reported dates for the measurements at Palomares (initially reported as Almeria), with a 4 $\mu Bq/m^3$ value from 25 May - 2 June, and a 890 value from 2-8 June. The model significantly over-estimated the first measurement, and missed the second. For subsequent model runs we switched the dates for these measurements because we believed the dates were incorrectly reported. The model also over-estimated the measurements in Austria, and Switzerland.

We did not attempt to match the Gibraltar measurements until the final set for two reasons:

- The exact locations for the release and many measurement locations were not available, and
- The source location description was inconsistent with the locations of the city of Algeciras and Gibraltar.

Time-series Comparison

Figure 11 shows a comparison of measured daily-averaged air concentrations to computed concentrations at Ispra for five consecutive days. Figure 12 compares values at three French sites for two consecutive days. The results are mixed. At Ispra the model lagged the observed peak by one day, but matches the area under the curve well.

For the French sites, the model generally over-estimated values but matched the measurement trend at Cadarache and Montpellier. We achieved good agreement with the measurement on 2 June at Nice, but over-predicted the value on 3 June. Due to the limited number of consecutive measurements at these sites, it is not clear why the results were mixed.

SET 2 SIMULATION

Model Grid

After releasing the Set 1 products, we continued to receive additional measurement data. With this increased data we decided to make another estimate that best matched all the data, not just the highest values. In order to include all the data, we expanded the model domain to 2600 km (Fig. 13) to include more of eastern and central Europe. This reduced the terrain resolution to 32.5 km, but this was still adequate to resolve the sea-level Gibraltar Strait (Fig. 14). We maintained the vertical dimension of 3 km.

Meteorological Data

As in Set 1 we used the one-degree NOGAPS data.

Dispersion Parameters

We used the same boundary layer heights as in Set 1, but decreased the daytime boundary layer to 1000 m, and increased the evening transitional period to 750 m. We also adopted a slightly unstable stability class for the daytime period.

Source Term Assumptions

Model iterations indicated that the release was probably much shorter than 12 hr. We estimated a 30 min release of 50 Ci from 1500 UTC (1300 local) to 1530 UTC (1330 local) on 29 May (in the middle of the 12-hour release time used for Set 1) best fit the measurements. We used the stack and particle size parameters as in Set 1.

Results

Figure 15 shows that the Set 2 one-day average air concentration was similar to the Set 1 pattern. The first two days closely match (Fig 15a-b), and on 1 June (Fig. 15c) spotty concentrations greater than 100 $\mu Bq/m^3$ are analyzed over central Italy, with contours greater than 10 $\mu Bq/m^3$ appearing over former Yugoslavia. This is due to rapidly transported, elevated sections of the plume mixing downward to the surface.

On 2 June (Fig. 15d) high concentrations are evident over central Italy. With the smaller released amount, the areas of highest concentrations are slightly smaller than Set 1. The effect of reducing the release duration from 12 hr to 30 min appears small.

Figure 16 shows the first 7-day average surface air concentration. As with the initial Set 1 calculations, the axis of the footprint remains over the Mediterranean Sea, although with about equal sections passing north and south of the Alps. The footprint extends from eastern Spain northward over central France, then northeastward over central Germany and

the Czech Republic. The eastern section of the plume covers all of Italy except Sicily, as well as the Balkans, Romania and Bulgaria.

Appendix 2 indicates the Set 2 model results compared well with measurements. Overall almost 44% of the 58 above-detection threshold measurements available at that time are predicted within a factor of two, 74% within a factor of five and almost 90% within a factor of ten. The reduced source strength more closely matches the highest measurements at Nice and Montpellier, but is worse for Cadarache and Toulon. There is a bias toward model over-prediction. Nearly all of the missed measurements (zero computed versus a greater than detection threshold measurement) are associated with small measured values at the edge of the plume. In the case of distant sites such as Orsay, the missed values are most likely due to the MATHEW code producing transport winds which are too slow (under-advection). The model also produced concentrations later than the reported measurements (not shown).

Time-series Comparison

Figure 11 shows that Set 2 did not produce significantly different daily comparisons at Ispra than Set 1, although plume arrival over central Italy occurs on 01 June. The one-day delay at Ispra could be due to slightly offset (to the south of northern Italy) direction of transport of the elevated plume or the above mentioned model under-advection. Results at Montpellier and Nice (Fig. 12a, c) are similar to Set 1, but higher concentrations were computed for 3 June. Higher than measured concentrations for both days were computed at Cadarache (Fig. 12b).

SET 3 SIMULATION

Source Term Assumptions

On 30 June, CSN provided ARAC with detailed information including the exact location of the Acerinox plant, as well as stack parameters. This location was about eight km west from our initial estimate (Fig. 2).

Additionally, CSN indicated the most likely release rate was 8-80 Ci between 0100 UTC (0300 local) and 0300 UTC (0500 local) on 30 May. We assumed a 50 Ci release of 30 minute duration commencing at 0130 UTC on 30 May 1998.

Model Grid

We used the same 2600 km grid as in Set 2.

Meteorological Data

Since we had specific source information, we decided to blend WMO surface and upper air observations with the gridded meteorological data. We added observations to the gridded data for coastal areas of the western Mediterranean for the first four days of the simulation (until most of the model plume was over southern Europe). We used the

observations to clarify flow near the source, and to improve the representation of coastal influences on the edge of the plume.

Figure 17 shows near-surface wind patterns of the combined observed and gridded data. Figure 17a shows the pattern at 0130 UTC on 30 May is similar to the one produced by gridded data alone, but relatively stronger winds prevail in Gibraltar Strait (the winds in the Strait were poorly resolved by the gridded data). The wind vectors affecting the plume for the next three days (Fig. 17b-d) are similar to the winds produced by gridded meteorological data alone. When compared with Figure 8, Figure 18 shows that the sparse upper air observations had little effect on the 1500 m wind pattern.

Dispersion Parameters

We continued to refine our boundary layer heights and stability inputs. We changed the time periods from 6-hr intervals to a 9-hr daytime period from 0900 to 1800 UTC, a nighttime period from 2100 to 0500 UTC, and 3-hr afternoon and 4-hr morning transitional periods. We used observed upper-air sounding data from stations near the Mediterranean that were closest to the plume center to determine boundary layer heights. As the plume was mostly over the continent after four days, we modified boundary layer heights to reflect continental effects. We increased the heights to 1700 m for daytime, to 1000 m for the evening transition, and 500 m at night and for the morning transition.

We returned to a neutral daytime stability as in Set 1 while the plume was over the Mediterranean Sea. Also we decided to use a slightly stable stability class at night. After four days, when the plume was mostly over the continent, we also used a slightly unstable stability class for the daytime.

Results

Figure 19 shows that the calculated surface concentrations were similar to the previous two sets. Figure 19a and 19b are close to the results of previous sets, but as of 1200 UTC on 2 June (Fig. 19c) higher concentrations prevail over Italy and former Yugoslavia. On the fourth day (Fig 19d), the highest concentrations are mostly over land, primarily southern France and much of Italy. Figure 20 shows the axis over the Mediterranean Sea to the southeast of the Balearic Islands. The western and northern geographic extent are similar to the previous runs, most likely associated with mid- to low-level transport. However, the eastern edge of the plume, particularly over the central Mediterranean, shows a significant increase in concentrations. This is due to the slightly more rapid transport in Set 3, resulting in greater extent south of the Alps.

Appendix 2 lists the ratios of measured to computed air concentrations at over 70 locations with 117 measurements. Statistical evaluation of Set 3 results indicate the model computed air concentrations were within a factor of two 37%, a factor of five 63%, and a factor ten, 73% of the time. These percentages are slightly lower than for Set 2 due to additional low measured concentrations added to the data set. However, the over-estimate bias was greatly reduced. Accuracy improved for Toulon, Nice (first day), and Montpellier, and was unchanged at Cadarache.

The longer duration average measurements in northern Italy are more accurately modeled than one-day averages. Comparisons of one-day measurements at Ispra, Vercelli,

Torino and Capo Mele show larger errors than comparison with measurements for multiple days at other locations. No other clear regional bias is evident.

Time-series Comparison

Figure 11 shows Set 3 produced lower modeled peak concentrations, and overall less area under the curve, compared to the other sets at Ispra. The one-day lag due to either slow transport, or small direction error, remains. Figure 12 shows the model improved over previous sets at all three French locations. Figure 21 shows the model computed air concentrations at three Italian locations, Vercelli, Capo Mele and Torino. Only two one-day averages are available at each site, but in every case the measured highest value occurs one day prior to the computed peak. This is consistent with the one-day delay with the Ispra time series data, and is consistent with higher model errors for one-day measurements versus longer period measurements. A delay in the arrival of material at a measurement site is averaged out in longer period measurements, but is apparent in the daily measurement data.

We also tried adjusting the release time provided by the Spanish Government forward in time; however, this test produced worse results both compared to the Ispra daily data and overall statistics (not shown).

Comparisons with previous studies

ARAC's models have been previously evaluated on the continental scale (2000-5000 km) against four tracer and measurement data sets listed below. For the first, rawinsonde observations were used to initialize the wind field, for the other three prognostic model gridded data were used. We blended four days of observations with the prognostic data for the Algeciras simulation.

Table 2. Summary of continental scale ARAC model simulations.

Experiment - Event	Meteorological input	Duration (days)	Scale (km)	Air concentration sampler averaging time
CAPTEX	Observations	2-3	1000	6-hr
ANATEX	NGM	5-7	2000	24-hr
ATMES	ECMWF	14	5000	6- & 24-hr
ETEX	ECMWF 0.5 deg	2	2500	3-hr
ALGECIRAS	NOGAPS 1.0 deg + observations	20	2600	1- to 20-days

Several factors are involved in comparing the current study to previous model evaluations. First is model evaluation protocol -- how the model output is compared with the measured air concentrations. The most stringent test is to pair the model output in both space and time to the measurements. This protocol was used in this study. Since concentrations from the CAPTEX and ANATEX experiments were not paired in time, those results are not compared with the Algeciras study. The ATMES and ETEX evaluations are comparable reference experiments which use the stringent time and space paring.

The second factor involved in comparing the current study to previous ones is the averaging time of the measured air concentrations. A shorter averaging time makes for a

more challenging model evaluation. For contintental scale experiments measurement averaging times are typically 3 to 24 hr. In order to compare our Algeciras results to previous studies, we selected only the shortest or 24-hr average air concentrations. This reduced the number of measurements from 117 to 24.

The third factor to consider when comparing model evaluations is the quality of the data set. For controlled tracer experiments, a significant number of samples are distributed in space and time to provide enough data to make statistically significant estimates of model accuracy during plume passage. The Algeciras data set was built from routinely available monitoring data, most of which was multi-day samples. The 24-hr average Algeciras comparison data set is limited to 24 samples taken only in France and Italy. Consequently any comparisons to the higher quality tracer data sets are at best weak.

Figure 22 summarizes the mean ratio of observed to modeled concentrations for each of the continental model evaluation data sets. The "n" values indicate the number of pairs matched in space and time. The 24 Algeciras 24-hr values were computed to be within a factor of two 50%, a factor of five 71%, and a factor of ten 79% of the 24 measured values. This limited data set indicates that these results may be comparable to previous studies, this comparison cannot be taken as statistically significant.

Dose Calculation

Based upon the Set 3 source term, we estimated the whole-body dose due to ground shine from deposited Cs-137 after 20 days exposure (Fig. 23). The highest contour calculated, 10^{-8} Rem (10^{-4} μSv), is well below any health effect. The pattern is similar to the 7-day average air concentrations, both in geographic coverage and the highest values over the Mediterranean Sea. Of course ground shine for deposition over water areas is irrelevant except in the case of material deposited on ships and not removed by rain or deck wash.

SUMMARY

We used the ARAC emergency response modeling system to simulate the accidental release of Cs-137 from a steel mill in southern Spain near Gibraltar. The Algeciras accident provides an excellent real-world case study for developing a source term based on sparse measurements. Without knowing the exact location, we used gridded meteorological data and a small set of sparse air concentration measurements to estimate the time and amount of the release. In all we made several model runs each based on more information about the incident. Initial model results showed the plume traveled mostly over the western Mediterranean Sea until it arrived in Central Europe. Initially we estimated a 100 Ci release over 12 hr on 29 May (0900-2100 UTC).

After receiving more air concentration data at greater downwind distances, we made two additional model runs using a 30 min release duration. For our third set of calculations we blended observed meteorological data with gridded data and produced the best comparison with the limited measurements.

Our 50 Ci source term for the third set compared favorably with the estimate provided by the Spanish Government of 8-80 curies released sometime between 0100-0300 UTC (0300-0500 local).

All model runs over-predicted the weekly-average measurements in Germany and Austria. Daily-average measurements over Italy indicates the calculated plume arrived one day late. This is due to our diagnostic wind model possibly producing slower transport than actually occurred. Comparison in other regions shows no clear bias.

One inconsistency is that our model indicates significant air concentrations on the Balearic Islands where measurements at a single location indicate below detection threshold air concentrations. We could not resolve the inconsistency between a good fit to data in central Europe and the large difference at the Balearic site.

Additionally, comparisons at close-in Palomares and Gibraltar sites are not good. Due to the strong concentration gradients, a slight deviation in modeled wind direction produces sharply different concentrations near the source.

Acknowledgment

This research was performed under the auspices of the U.S. Department of Energy Lawrence Livermore National Laboratory Contract No. W-7405-ENG-48.

REFERENCES

ARAC 1996: User's guide to the CG-MATHEW/ADPIC models. UCRL-MA-103581 Rev. 4, Lawrence Livermore National Laboratory, Livermore, CA, 255 pp.

Lange, R. and Foster, C.S., 1992. The Chernobyl ^{137}Cs release as a tracer experiment for long range transport and diffusion model within ATMES. UCRL-JC-111563, Lawrence Livermore National Laboratory, Livermore, CA, 31 pp.

Pace J.C., and Nasstrom, J.S., 1997: ARAC results from phase II of the European Tracer Experiment. *Proc. Amer. Nuclear Soc. Sixth Topical Meeting on Emergency Preparedness and Response,* San Francisco, CA, 521-524.

Rodriguez, D.J., 1987: A particle-in-cell technique for simulating the long range transport of pollutants. UCRL-98418, Lawrence Livermore National Laboratory, Livermore, CA, 19 pp.

_____, and Cederwall, R.T., 1990: A preliminary evaluation of ADPIC model performance on selected ANATEX releases using observed, analyzed and dynamically predicted winds. *Air Pollution Modeling and its Applications, VIII.* H. van Dop and D.B. Steyn, Eds., Plenum Press, 439-446.

Sullivan, T.J., Ellis, J.S., Foster, C.S., Foster, K.T., Baskett, R.L., Nasstrom, J.S. and Schalk, W.S., 1993: Atmospheric Release Advisory Capability: Real-time modeling of airborne hazardous materials. *Bull. Amer. Meteor. Soc..*, **74**, 2343-2361.

Appendix 1. Measurement locations used in each set

COUNTRY Site Name	Location	ARAC sets in which the measurement was used
FRANCE		
Toulan/ La Seyne	43° 07' N 05° 55' E	1-3
Charleville Mizihres	49.133° N 04.117° E	2-3
Orsay	49.117° N 02.033° E	2-3
Nice	43.700° N 07.250° E	1-3
Cadarache	43.683° N 05.700° E	1-3
Montpellier	43.600° N 03.883° E	1-3
Montfaucon	45.167° N 04.300° E	1-3
Marcoule	44.817° N 04.700° E	2-3
Dijon	47° 19' N 05° 01' E	3
Bordeaux	44.883° N 00.567° W	3
SPAIN		
Palomares	37.250° N 01.783° W	1-3
Madrid	40.400° N 03.683° W	1-3
Gibraltar	36.118° N 05.337° W	1-3
Valencia (Cofrentes NPP)	39.233° N 01.067° W	2-3
GERMANY		
Freiburg/Schauinsland	49.920° N 07.900° E	2-3
Braunschweig	52.250° N 10.500° E	2-3
Mainz	50.000° N 08.200° E	2-3
Zugspitz	47.421° N 11.000° E	3
Freiburg	48.000° N 07.850° E	3
Garmisch	47.500° N 11.080° E	3
Konstanz	47.670° N 09.220° E	3
Munich	48.130° N 11.580° E	3
Stuttgart	47.780° N 09.200° E	3
AUSTRIA		
Vienna	48.217° N 16.333° E	1-3
Retz	48.750° N 15.950° E	1-3
Innsbruck	47.267° N 11.400° E	2-3
Linz	48.300° N 14.300° E	1-3
Salzburg	47.800° N 13.033° E	1-3
Graz	47.083° N 15.450° E	2-3
Bad Radkersburg	46.683° N 15.983° E	2-3
Klagenfurt	46.633° N 14.333° E	2-3

Appendix 1, continued.

COUNTRY Site Name	Location	ARAC sets in which the measurement was used
ITALY		
Milano	45.470° N 09.200° E	1-3
Ispra	45.817° N 08.617° E	1-3
Vercelli	45° 19' N 08° 25' E	3
Ivrea	45° 28' N 07° 52' E	3
Torino	45° 03' N 07° 22' E	3
Capo Mele	43° 57' N 08° 10' E	3
Genoa	44° 25' N 08° 57' E	3
Arenzano	44° 24' N 08° 41' E	3
Cogoleto	44° 23' N 08° 39' E	3
Savona	44° 17' N 08° 30' E	3
La Spezia	44° 07' N 09° 50' E	3
Udine	46° 03' N 13° 14' E	3
Verona	45° 27' N 11° 00' E	3
Villa Franca	45° 21' N 10° 50' E	3
Belluno	46° 09' N 12° 13' E	3
Mestre-Venice	45° 29' N 12° 15' E	3
Trino	45° 12' N 08° 18' E	3
Caorso	45° 03' N 09° 52' E	3
Saluggia	45° 14' N 08° 00' E	3
Piacenza	45° 01' N 09° 40' E	3
Parma	44° 48' N 10° 20' E	3
Reggio Emilia	44° 43' N 10° 36' E	3
Monte Cimone	42° 24' N 12° 12' E	3
Bologna	44° 29' N 11° 20' E	3
Imola	44° 21' N 11° 42' E	3
Forli	44° 13' N 12° 03' E	3
Capo Caccia	40° 34' N 08° 09' E	3
Tarquinia	42° 15' N 11° 45' E	3
Palermo	38° 07' N 13° 21' E	3
NETHERLANDS		
Bilthoven	52.117° N 05.200° E	2-3
SWITZERLAND		
Monte Ceneri	46.130° N 08.920° E	1-3
Geneva	46.230° N 06.050° E	1-3
Guttingen	47.600° N 09.280° E	2-3
Oberschrot	46.750° N 07.270° E	2-3

Appendix 1, completed.

COUNTRY Site Name	Location	ARAC sets in which the measurement was used
CZECH REPUBLIC		
Hradec Kralove	50.210° N 15.830° E	2-3
Plzeo	49.750° N 13.380° E	2-3
Prague	49.650° N 13.820° E	2-3
Eeske Budijovice	48.985° N 14.481° E	2-3
Brno	49.190° N 16.600° E	2-3
Ostrava	49.840° N 18.287° E	2-3
Dukovany NPP	49.030° N 16.120° E	2-3
Temelin NPP	49.170° N 14.420° E	2-3
HUNGARY		
Budapest	47.500° N 19.050° E	2-3
SLOVENIA		
Lubljana	46.067° N 14.500° E	2-3
SLOVOKIA		
Mochovce	48.260° N 18.450° E	3
Bohunice	48.470° N 17.683° E	3

Appendix 2 Comparison of measured to computed Cs-137 air concentrations

			Set 1		Set 2		Set 3	
Site Name	Averaging Period	Meas. (μBq/m^3)	Comp. (μBq/m^3)	Meas./ Comp.	Comp. (μBq/m^3)	Meas./ Comp.	Comp. (μBq/m^3)	Meas./ Comp.
Toulon/ La Seyne[1]	25 May-2 June	2430	1010	2.41	456	5.33	554	4.48
	2 - 6 June	200	596	0.34	394	0.51	343	0.58
	5 - 10 June	5.5	-	-	-	-	4.98	1.10
	10 - 15 June	2.9	-	-	-	-	0	missed
Charleville Mizitheres	25 May-2 June	19	-	-	0.04	533	0.09	224
	31 May-5 June	22	-	-	-	-	3.12	7.05
	5 - 10 June	3.0	-	-	-	-	2.53	1.18
Orsay	25 May-2 June	3.8	-	-	0	missed	0	missed
	2 - 5 June	3.39	-	-	-	-	1.86	1.82
	5 - 10 June	1.10	-	-	-	-	7.10	0.16
Nice	1 - 2 June[2]	2100	2360	0.83	2480	0.85	1580	1.33
	2 - 3 June[2]	330	-	-	3110	0.11	3220	0.10
Cadarache	1 - 2 June[2]	1600	3730	0.429	2900	0.55	2980	0.54
	2 - 3 June[2]	510	-	-	1760	0.29	1570	0.33
Montpellier	1 - 2 June[2]	600	2890	0.21	1630	0.34	1300	0.46
	2 - 3 June[2]	460	-	-	1050	0.44	797	0.58
Montfaucon	2 - 3 June[2]	870	-	-	653	1.33	646	1.35
Marcoule	1 - 2 June[2]	560	-	-	1280	0.44	838	0.67
Dijon	31 May-10 June	37.7	-	-	-	-	40.0	0.94
Bordeaux	29 May-10 June	2.12	-	-	-	-	9.84	0.22
Palomares	25 May-2 June[3]	890	2540	0.35	847	1.05	220	4.04
	2 - 8 June[3]	4	0	missed	0	missed	5.1E-03	779
Madrid	1 - 8 June	4	2.6E-3	1.6E+3	0	missed	0	missed
Valencia	25 May-2 June	11	-	-	0	missed	0	missed
Gibraltar	25 May-1 June	140	0	missed	0	missed	417	0.34
	1 - 8 June	40	0	missed	0	missed	0	missed
Freiburg/ Schauinsland	2 - 8 June	17.2	-	-	130	0.132	11.7	1.47

Appendix 2, continued.

			Set 1		Set 2		Set 3	
Site Name	Averaging Period	Meas. (μBq/m^3)	Comp. (μBq/m^3)	Meas./ Comp.	Comp. (μBq/m^3)	Meas./ Comp.	Comp. (μBq/m^3)	Meas./ Comp.
Braunschweig	2 - 8 June	2.1	-	-	9	0.23	20.7	0.10
Mainz	1 - 8 June	5.8	-	-	6.28	0.92	17.3	0.34
Zugspitze	1 - 8 June	21.8	-	-	-	-	124	0.18
Freiburg	1 - 8 June	11.5	-	-	-	-	78.4	0.15
Garmisch	1 - 8 June	13.3	-	-	-	-	113	0.12
Konstanz	1 - 8 June	13	-	-	-	-	62.6	0.21
Munich	1 - 8 June	9.4	-	-	-	-	59.7	0.16
Stuttgart	1 - 8 June	8.6	-	-	-	-	60.8	0.14
Vienna	1 - 8 June[4]	29	-	-	27.2	1.06	47.5	0.61
Retz	1 - 8 June[4]	22	-	-	23	0.96	38.1	0.77
Innsbruck	1 - 8 June[4]	98	-	-	52.3	1.87	128	0.77
Linz	1 - 8 June[4]	20	95.2	0.21	32.2	0.62	32.1	0.62
Salzburg	1 - 8 June[4]	14	156	0.09	78.7	0.18	67.3	0.21
Graz	1 - 8 June[4]	200	-	-	57.1	3.50	82.5	2.42
Bad Radkers-burg	1 - 8 June[4]	128	-	-	51.3	2.49	84.7	1.51
Klagenfurt	1 - 8 June[4]	174	-	-	130	1.34	138	1.26
Milano	1 - 3 June	1700	233	7.3	202	8.43	295	5.76
	1 - 2 June[2]	1780	-	-	-	-	1.97	905
	4 - 5 June[2]	215	-	-	-	-	424	0.51
Ispra	1 - 2 June[2,5]	390	0	missed	0.5	749	1.67	233
	2 - 3 June[2,5]	900	381	2.36	371	2.43	353	2.55
	3 - 4 June[2,5]	460	1010	0.46	726	0.63	662	0.70
	4 - 5 June[2,5]	140	171	0.82	597	0.24	87.1	1.61
	5 - 6 June[2,5]	150	28.0	5.36	102	1.48	11.0	13.6
	2 - 5 June	740	521	1.42	565	1.31	367	2.01
	29 May-5 June	220	-	-	242	0.91	158	1.40
	2 - 4 June	670	-	-	549	1.22	507	1.32
Vercelli	1 - 2 June[2]	1600	-	-	-	-	21.0	76.3
	2 - 4 June	1100	-	-	-	-	757	1.45
	4 - 5 June[2]	630	-	-	-	-	120	5.25
	6 - 7 June[2]	450	-	-	-	-	3.8	120
Ivrea	2 - 3 June[2]	600	-	-	-	-	962	0.62
	1 - 7 June	230	-	-	-	-	389	0.59
Torino	31 May-1 June[2]	240	-	-	-	-	0.73	330
	1 - 2 June[2]	1700	-	-	-	-	23.4	0.73

Appendix 2, continued.

			Set 1		Set 2		Set 3	
Site Name	Averaging Period	Meas. (μBq/m^3)	Comp. (μBq/m^3)	Meas./ Comp.	Comp. (μBq/m^3)	Meas./ Comp.	Comp. (μBq/m^3)	Meas./ Comp.
Capo Mele	1 - 2 June[2]	3220	-	-	-	-	1450	2.21
	2 - 3 June[2]	200	-	-	-	-	3240	0.06
Genoa	1 - 7 June	380	-	-	-	-	504	0.76
Arenzano	1 - 7 June	510	-	-	-	-	484	1.05
Cogoleto	1 - 7 June	800	-	-	-	-	488	1.64
Savona	1 - 7 June	730	-	-	-	-	534	1.32
La Spezia	4 - 8 June	320	-	-	-	-	8.66	37.0
Udine	1 - 7 June	31.2	-	-	-	-	165	0.19
Verona	30 May- 8 June	1000	-	-	-	-	211	4.73
Villafranca	30 May- 4 June	800	-	-	-	-	186	4.30
Belluno	1 - 8 June	800	-	-	-	-	234	3.42
Mestre-Venice	2 - 9 June	400	-	-	-	-	131	3.06
Trino	4 - 5 June	1000[6]	-	-	-	-	8.23	12.2
	5 - 6 June	1400[6]	-	-	-	-	2.89	485
	6 - 7 June	1700[6]	-	-	-	-	0.19	9.0E+4
	7 - 8 June	1200[6]	-	-	-	-	0	missed
Caorso	3 - 8 June	107[7]	-	-	-	-	227	0.62
Saluggia	21 May- 5 June	200	-	-	-	-	138	1.45
Piacenza	25 May- 7 June	180	-	-	-	-	151	1.19
Parma	29 May- 11 June	200	-	-	-	-	134	1.49
Reggio Emilia	27 May- 1 June	320	-	-	-	-	1.66	19.3
Monte Cimone	1 - 3 June	300	-	-	-	-	1260	0.24
Bologna	25 May- 7 June	180	-	-	-	-	133	1.35
Imola	26 May- 6 June	120	-	-	-	-	161	0.75
Forli	30 May- 5 June	250	-	-	-	-	277	0.90
Cappo Caccia	1 - 6 June	30	-	-	-	-	722	0.04

Appendix 2, continued.

			Set 1		Set 2		Set 3	
Site Name	Averaging Period	Meas. (μBq/m^3)	Comp. (μBq/m^3)	Meas./ Comp.	Comp. (μBq/m^3)	Meas./ Comp.	Comp. (μBq/m^3)	Meas./ Comp.
Tarquinia	1 - 5 June	60	-	-	-	-	493	0.12
	6 - 10 June	110	-	-	-	-	36.5	3.01
	11 - 15 June	110	-	-	-	-	0.68	161
Palermo	6 - 7 June[2]	76	-	-	-	-	98	0.77
Bilthoven	29 May-5 June	5.8	-	-	0	missed	4.9E-3	1.2E+3
Monte Ceneri	25 May-8 June	152	181	0.83	77.2	1.97	72.8	2.09
Geneva	25 May-2 June	31.5	93.2	0.34	86.2	0.37	38.5	0.82
	2 - 8 June	19	515	0.04	290	0.07	178	0.11
Guttingen	2 - 8 June	13	-	-	126	0.10	73.5	0.18
Oberschrot	25 May-8 June	6	-	-	119	0.05	82.8	0.08
Hradec	27 May-3 June	2	-	-	0	missed	0.19	10.8
	3 - 10 June	11	-	-	36.0	0.31	47.9	0.23
Plzeo	27 May-3 June	2.5	-	-	1.08	2.31	4.28	0.59
	3 - 10 June	3.7	-	-	61.2	0.06	44.4	0.08
Prague	26 May-2 June	0.9	-	-	0	missed	0	missed
	2 - 5 June	4.7	-	-	15.5	0.30	69.8	0.07
	5 - 9 June	11	-	-	26.2	0.42	49.8	0.22
	9 - 12 June	0.5	-	-	0	missed	2.13	0.24
Eeske	3 - 10 June	8.7	-	-	60.4	0.14	73.3	0.12
Brno	27 May-3 June	10.4	-	-	1.9E-3	5.6E+3	0.07	134
	3 - 10 June	26.2	-	-	24.0	1.09	54.8	0.48
Ostrava	1-8 June	56	-	-	15.9	3.51	37.8	1.48
Dukovany	1-7 June	13.5	-	-	18.8	0.72	35.7	0.38
Temelin	3 - 10 June	10.7	-	-	71.1	0.15	71.7	0.15
Budapest	2-8 June	100	-	-	74.1	1.35	95.2	1.05
Lubljana	1 - 10 June	243	-	-	106	2.29	126	1.93

Appendix 2, completed.

			Set 1		Set 2		Set 3	
Site Name	Averaging Period	Meas. (μBq/m^3)	Comp. (μBq/m^3)	Meas./ Comp.	Comp. (μBq/m^3)	Meas./ Comp.	Comp. (μBq/m^3)	Meas./ Comp.
Mochovce	29 May-5 June	26.3	-	-	-	-	12.0	2.2
	5 - 12 June	12.9	-	-	-	-	57.5	0.22
Bohunice	27 May-10 June	23.3	-	-	-	-	21.3	1.09
	10 - 17 June	26.1	-	-	-	-	24.9	1.05

Notes:

1. La Seyne sur Mer and Toulon were originally two different sites, and were later merged.
2. This portion of the data was used for the 24 hr matched-pair statistical comparison to previous continental scale ARAC simulations.
3. The dates for these two measurements were switched in order to be more consistent with the data.
4. The dates for the Austrian data were reported from 1-2 June through 8-9 June. ARAC selected a valid time from 1-8 June.
5. ARAC used the dates provided by direct communication with Ispra for the daily concentrations. An alternate data source reported the same measurements to be one day later.
6. The magnitude and timing of the measurement data at Trino is highly inconsistent with data at nearby sites reporting for the same general time period.
7. This value is the average of two measurements provided for the same time period at Caorso.

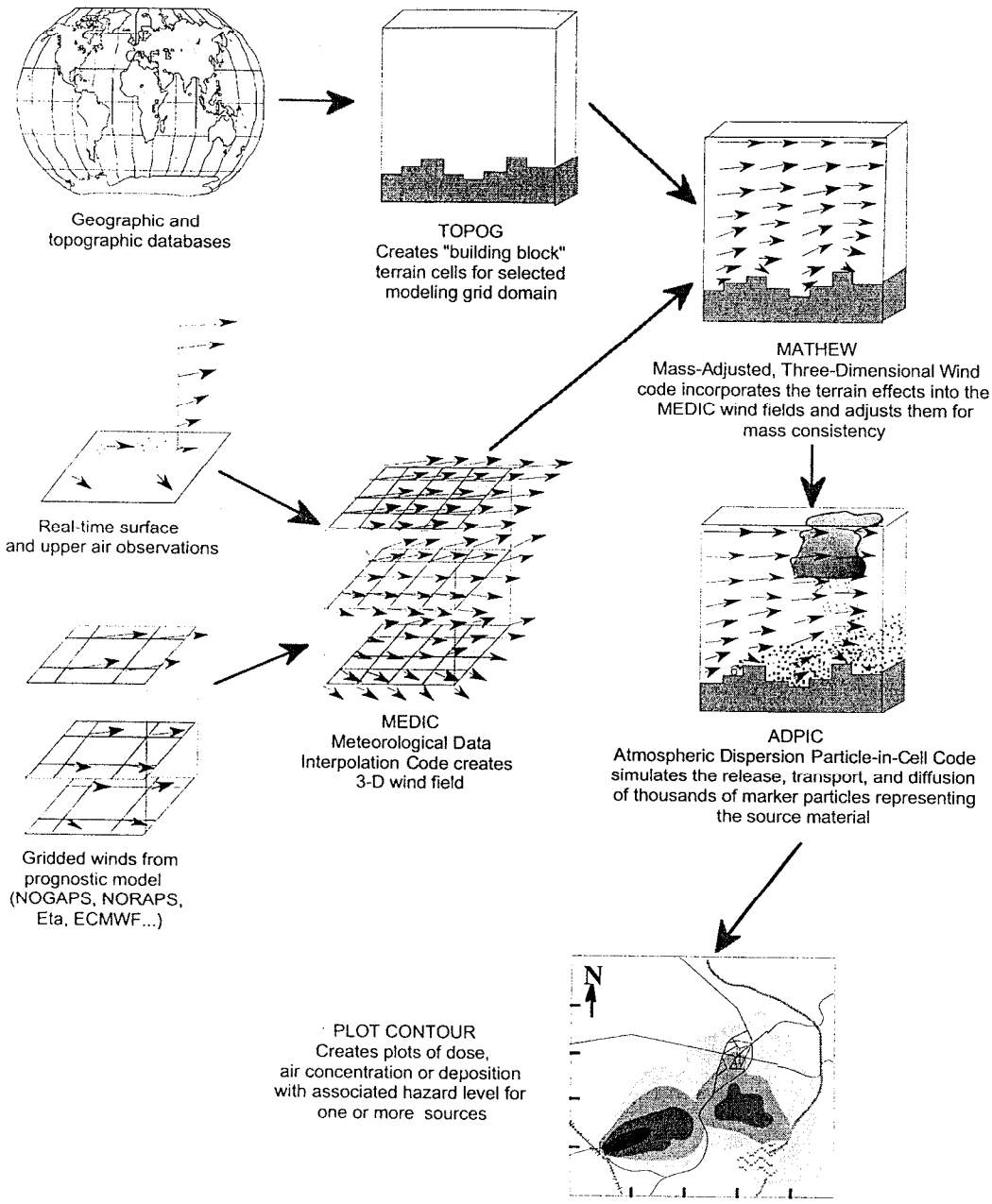

Figure 1. ARAC Emergency Response Modeling System

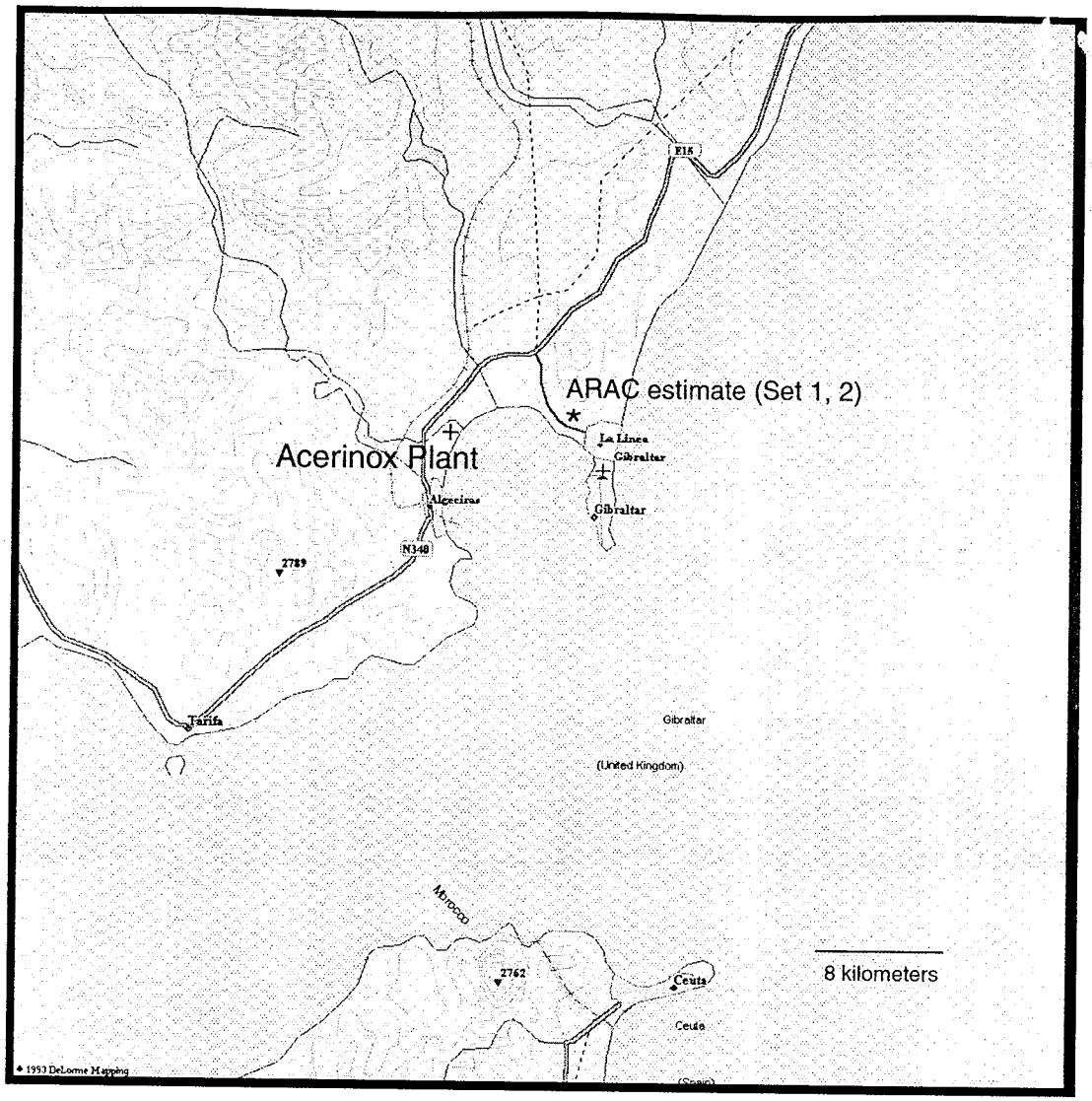

Figure 2. Map of the release locations.

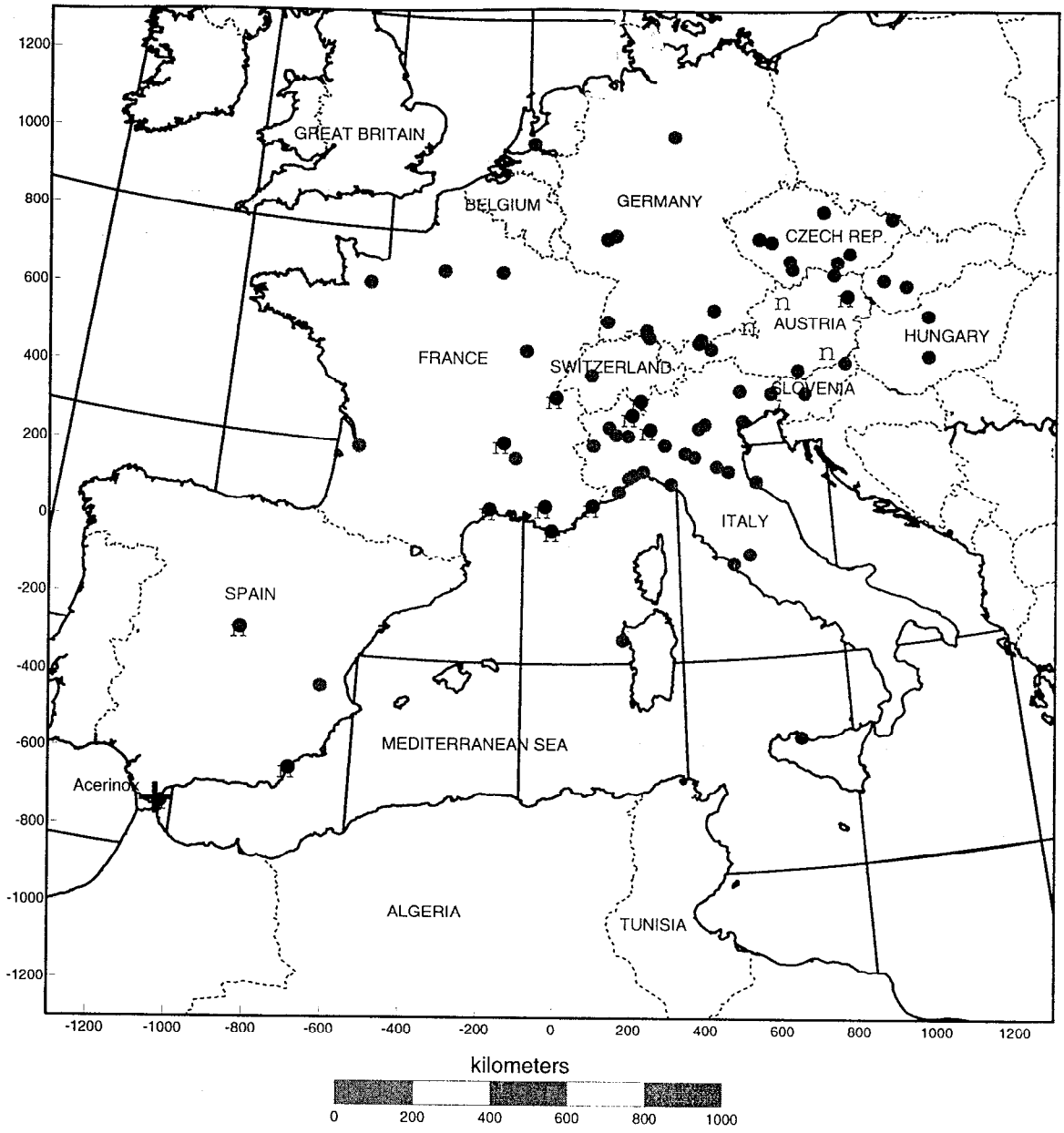

Figure 3. Measurement locations. Squares indicate measurements used to assess the initial source term, circles represent additional measurements used for Sets 2 or 3.

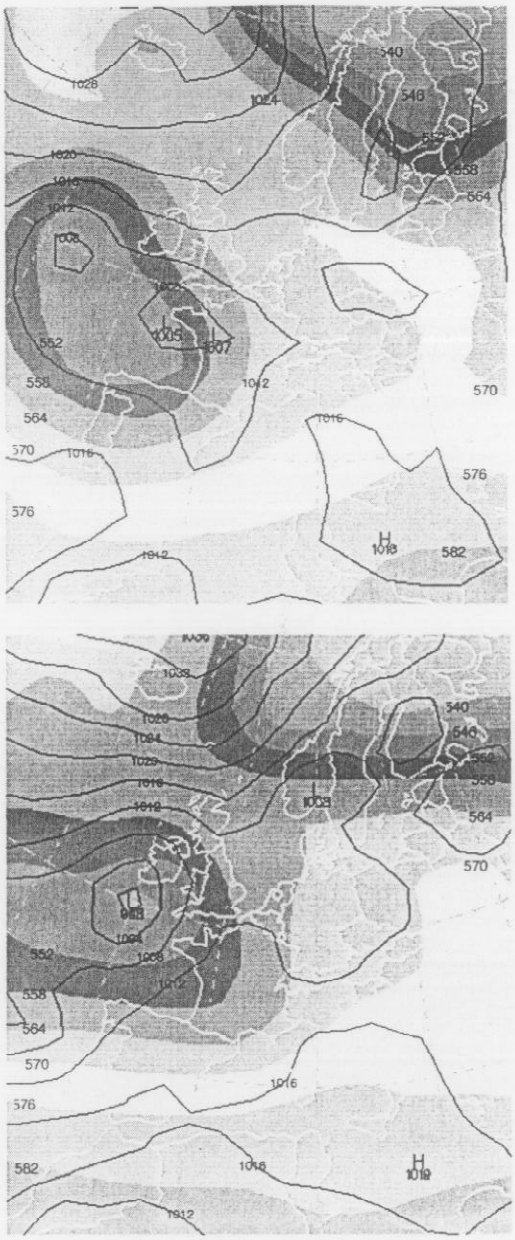

Figure 4. ECMWF analysis surface pressure contours (in mb) and 500 hPa heights (gray scale) for 1200 UTC on: (a) 30 May, and (b) 31 May 1998

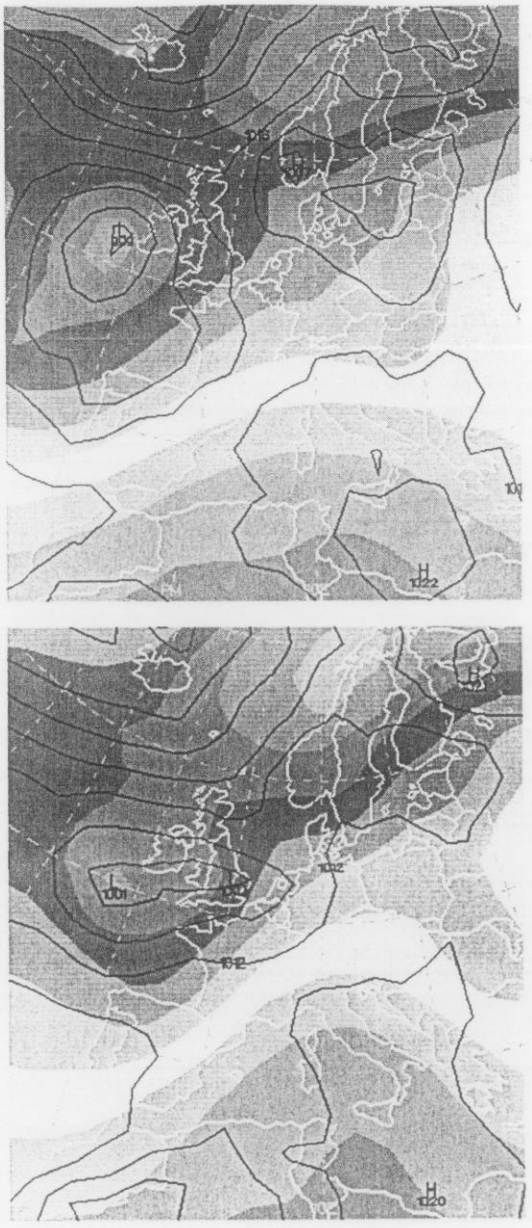

Figure 4. ECMWF analysis surface pressure contours (in mb) and 500 hPa heights (gray scale) for 1200 UTC on: (c) 01 June, and (d) 02 June 1998

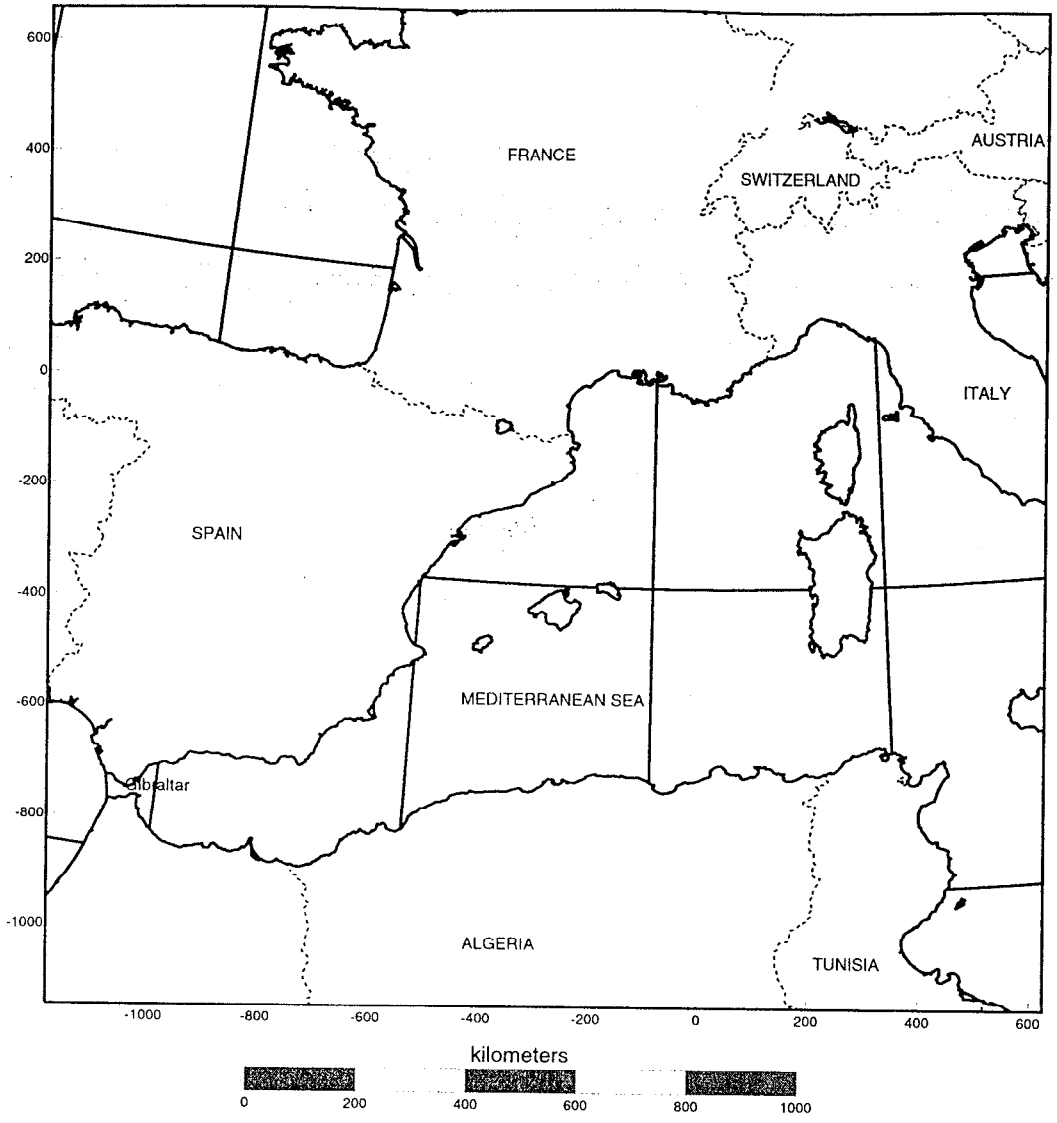

Figure 5. 1800 km model domain used for Set 1 (initial) products.

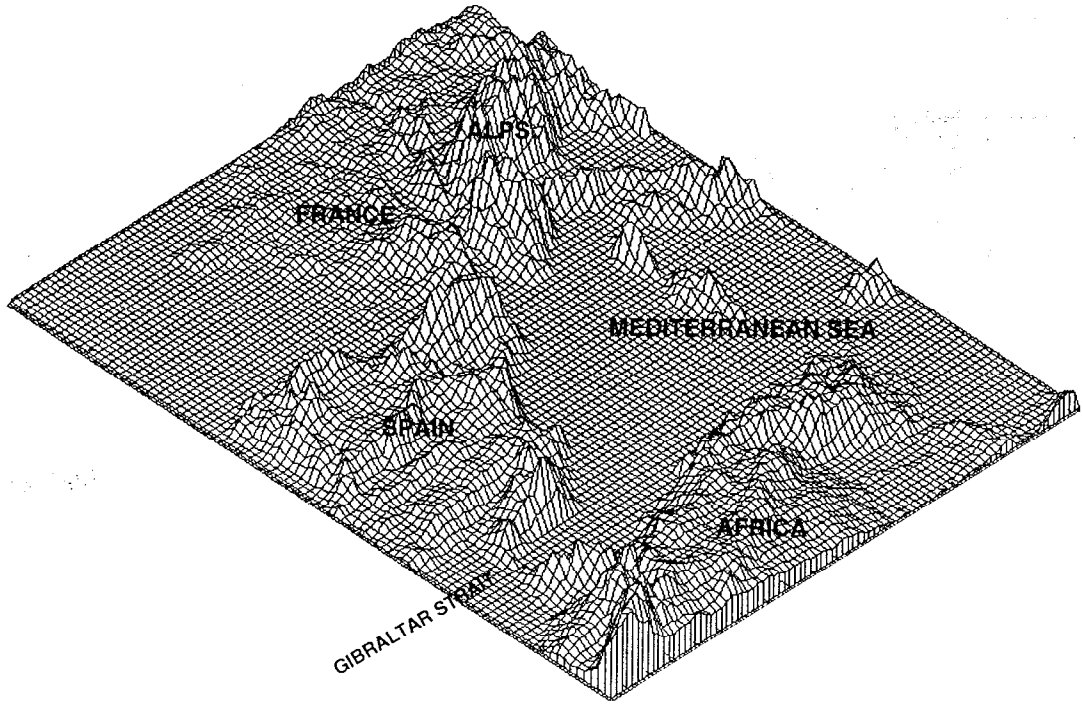

Figure 6. Perspective view of 1800 km terrain.

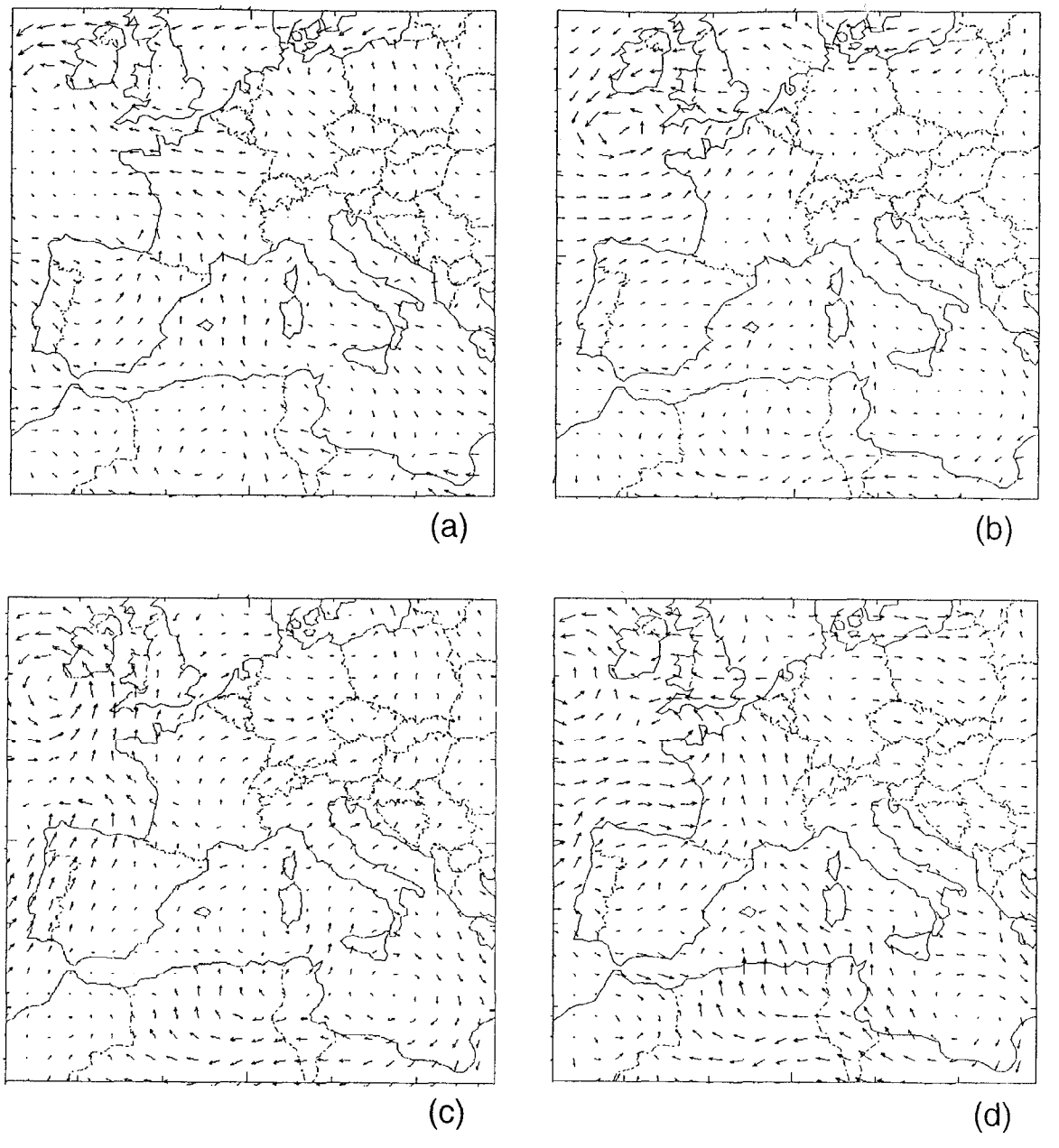

Figure 7. Set 1 near surface model wind vectors at 0300 UTC for (a) 30 May, (b) 31 May, (c) 1 June, and (d) 2 June 1998.

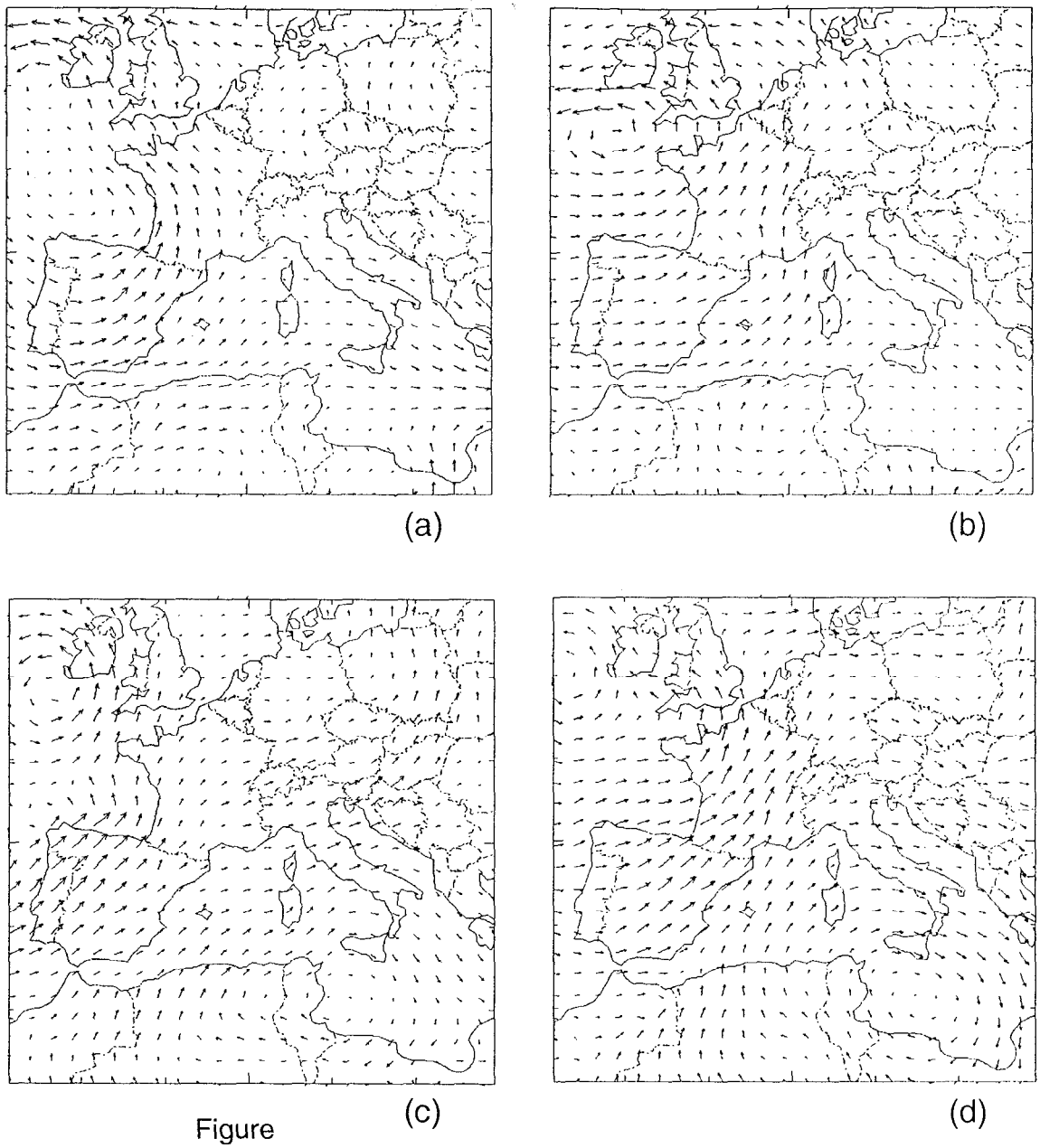

Figure

Figure 8. Set 1 model wind vectors at 1500 m above ground at 0300 UTC for (a) 30 May, (b) 31 May, (c) 1 June, and (d) 2 June 1998.

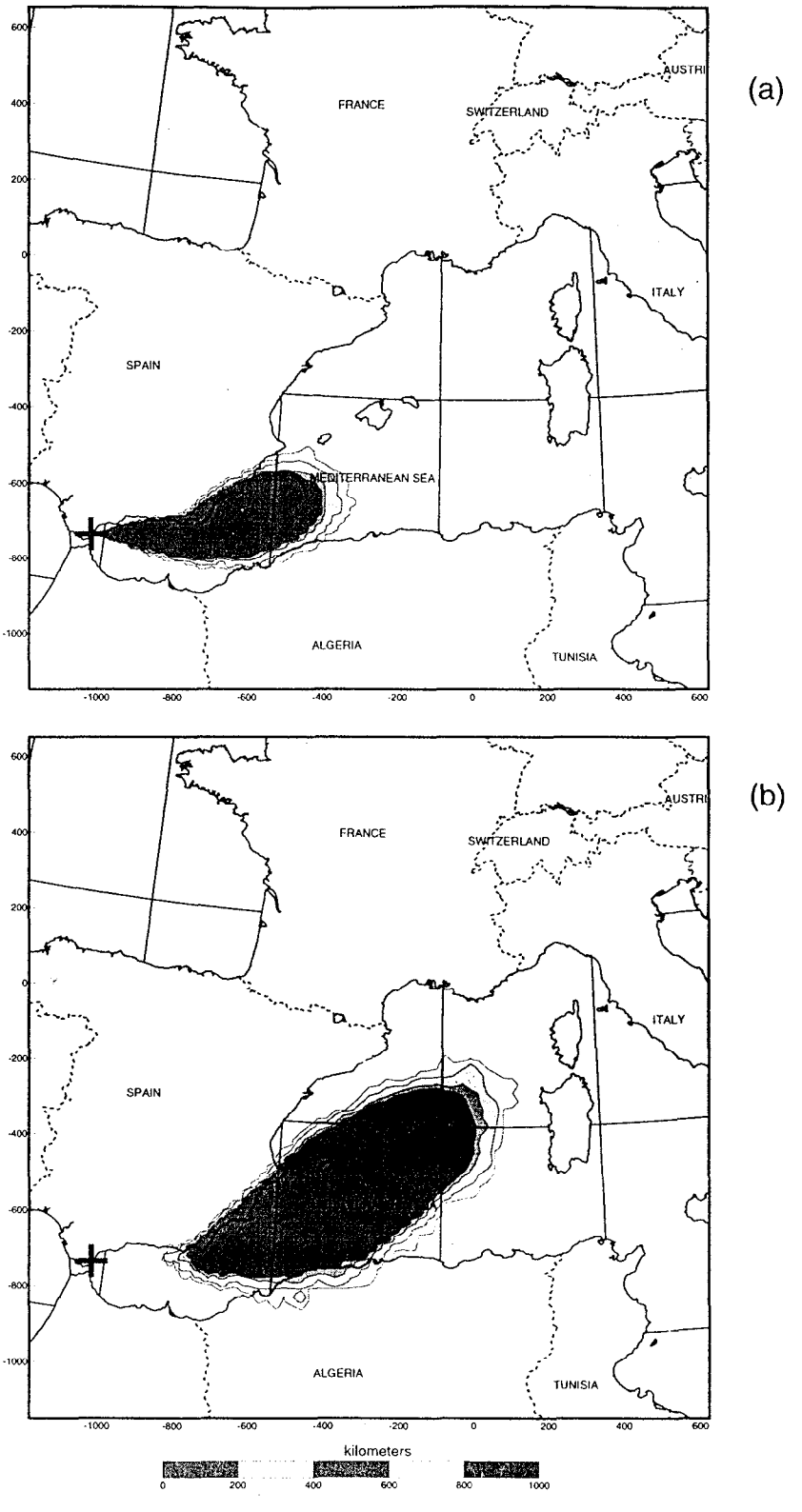

Figure 9. One-day average air concentration plots for Set 1 ending at 0900 UTC on (a) 30 May and (b) 31 May. Contours: >10 (outermost or lightest), >100, >500, and >1000 uBq/m3 (innermost or darkest).

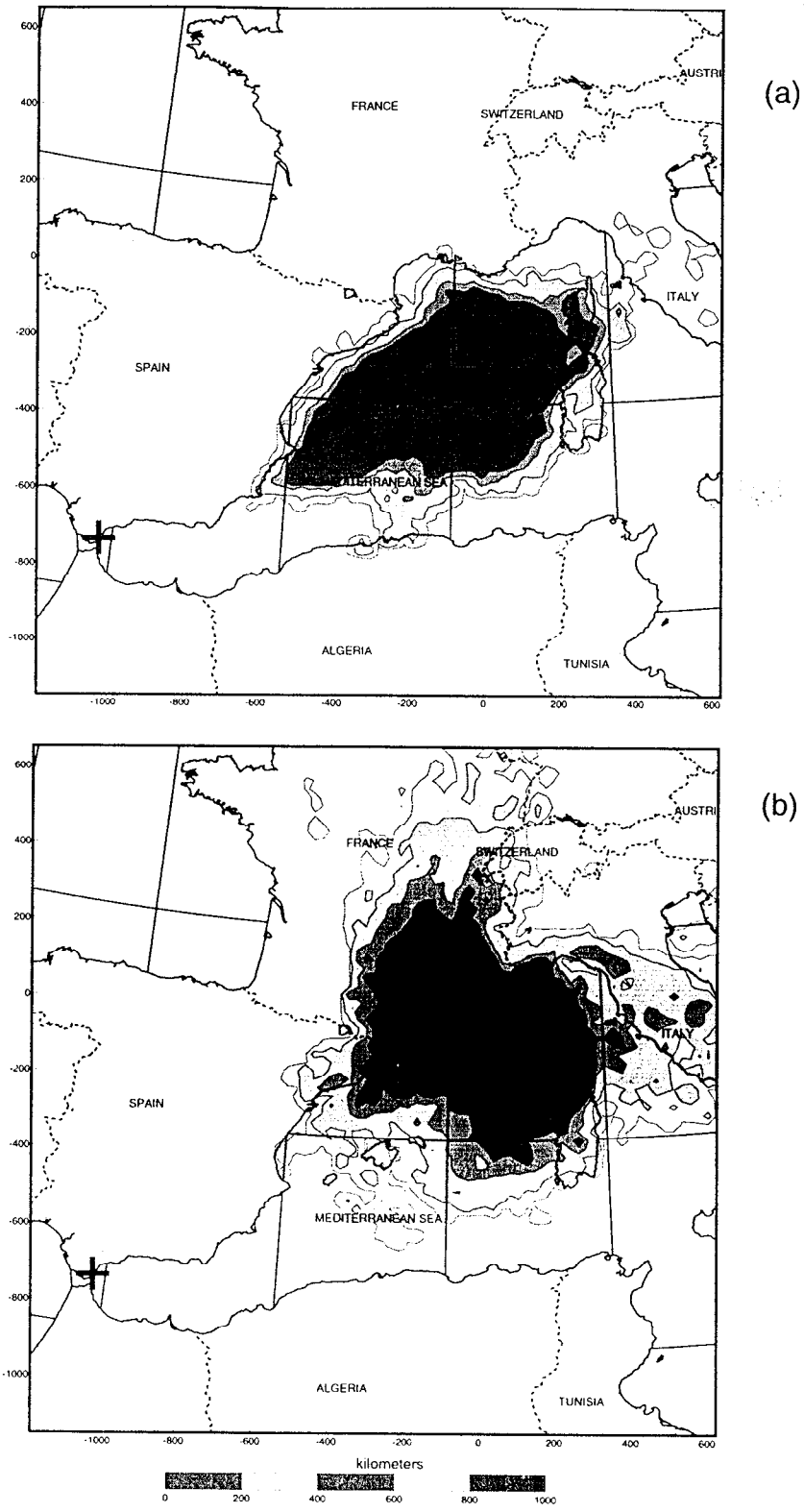

Figure 9 (continued). One-day average air concentration plots for Set 1 ending at 0900 UTC on (c) 1 June and (d) 2 June. Contours: >10 (outermost or lightest), >100, >500, and >1000 uBq/m3 (innermost or darkest).

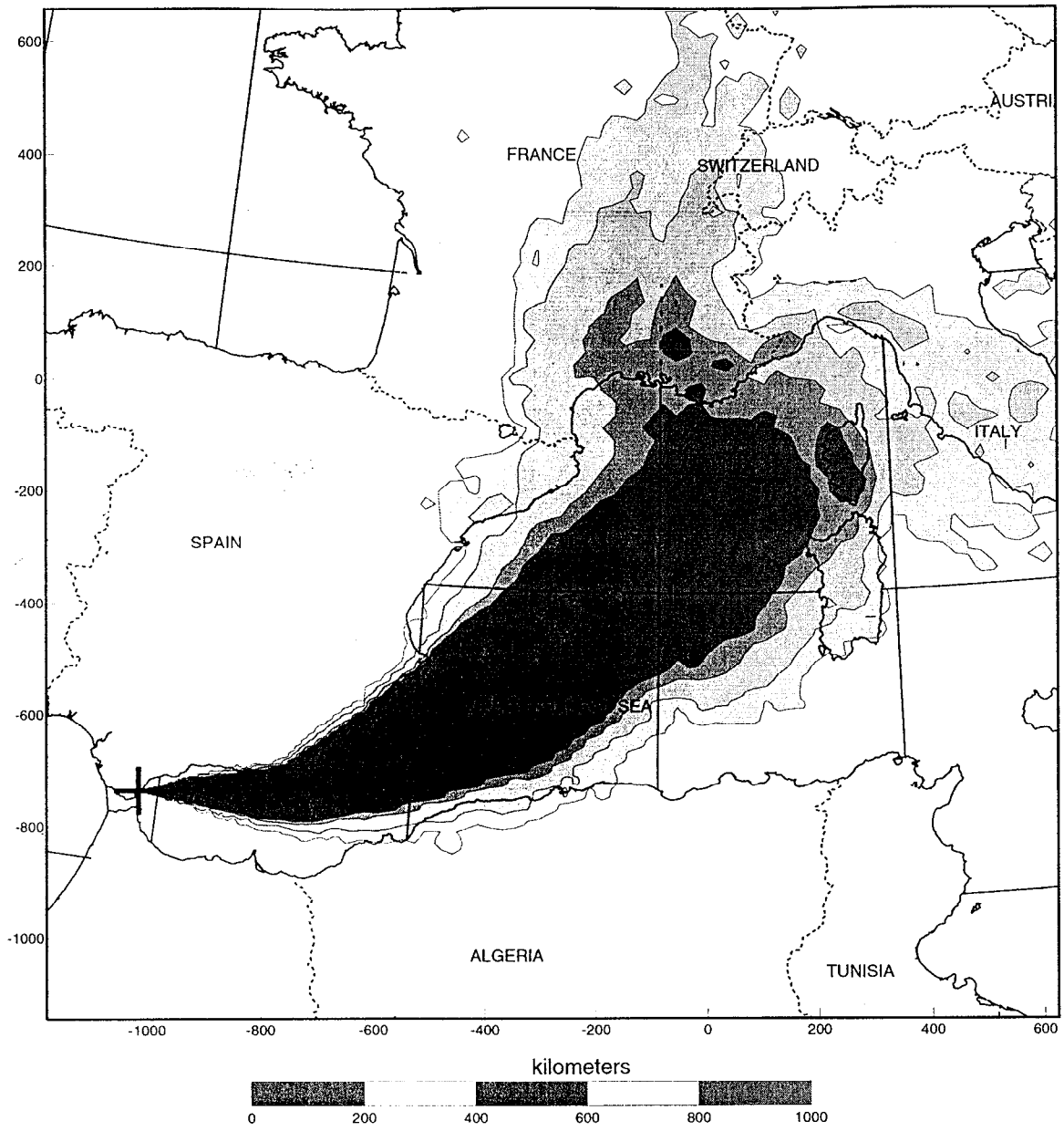

Figure 10. Five-day average air concentration plot for Set 1 ending at 0900 UTC on 2 June 1998. Contours: >10 (outermost or lightest), >100, >500, and >1000 uBq/m3 (innermost or darkest).

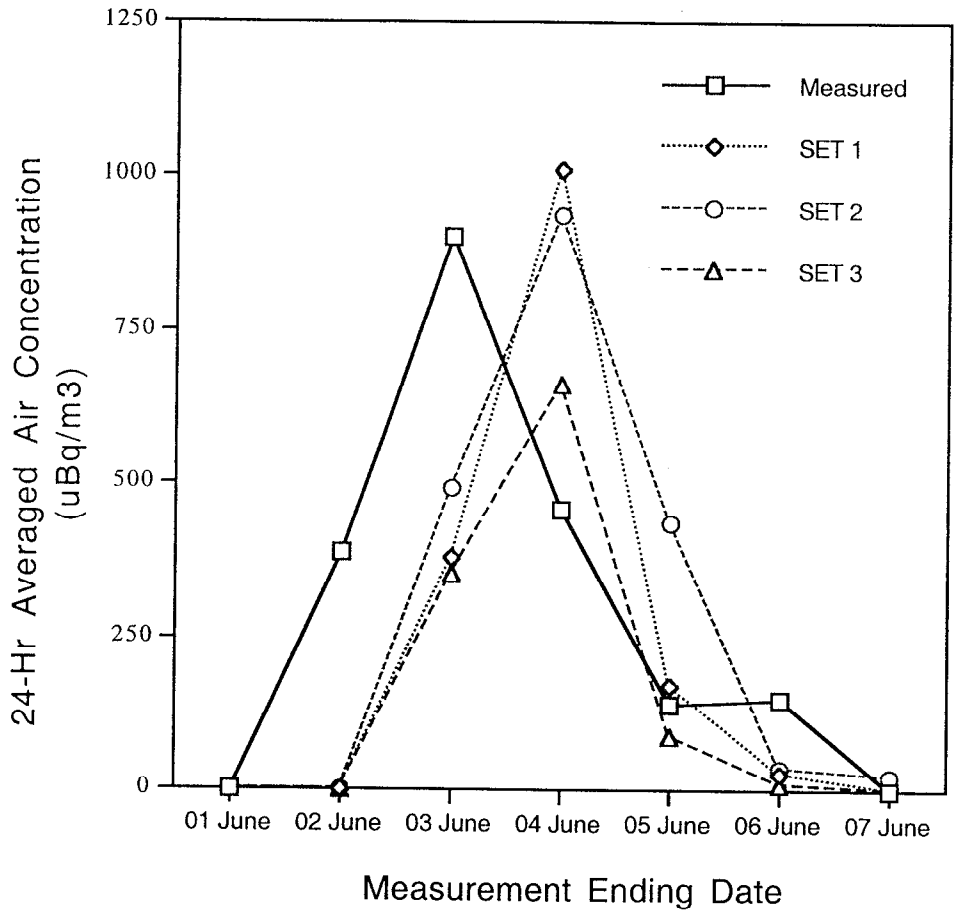

Figure 11. Comparison of computed with measured daily average air concentrations at Ispra, Italy for 1-7 June.

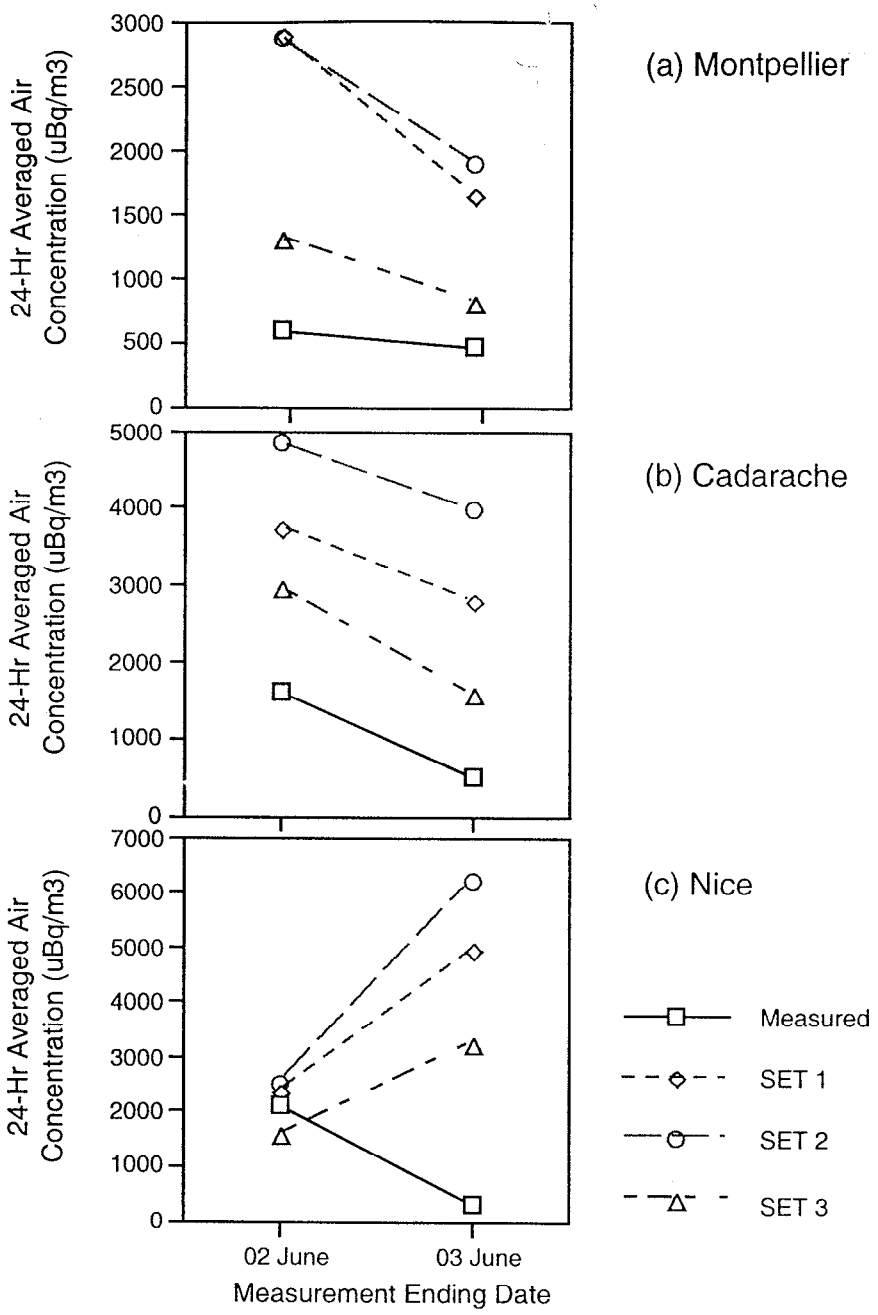

Figure 12. Comparison of computed with measured daily average air concentrations for 2-3 June at (a) Montpellier, (b) Cadarache and (c) Nice, France.

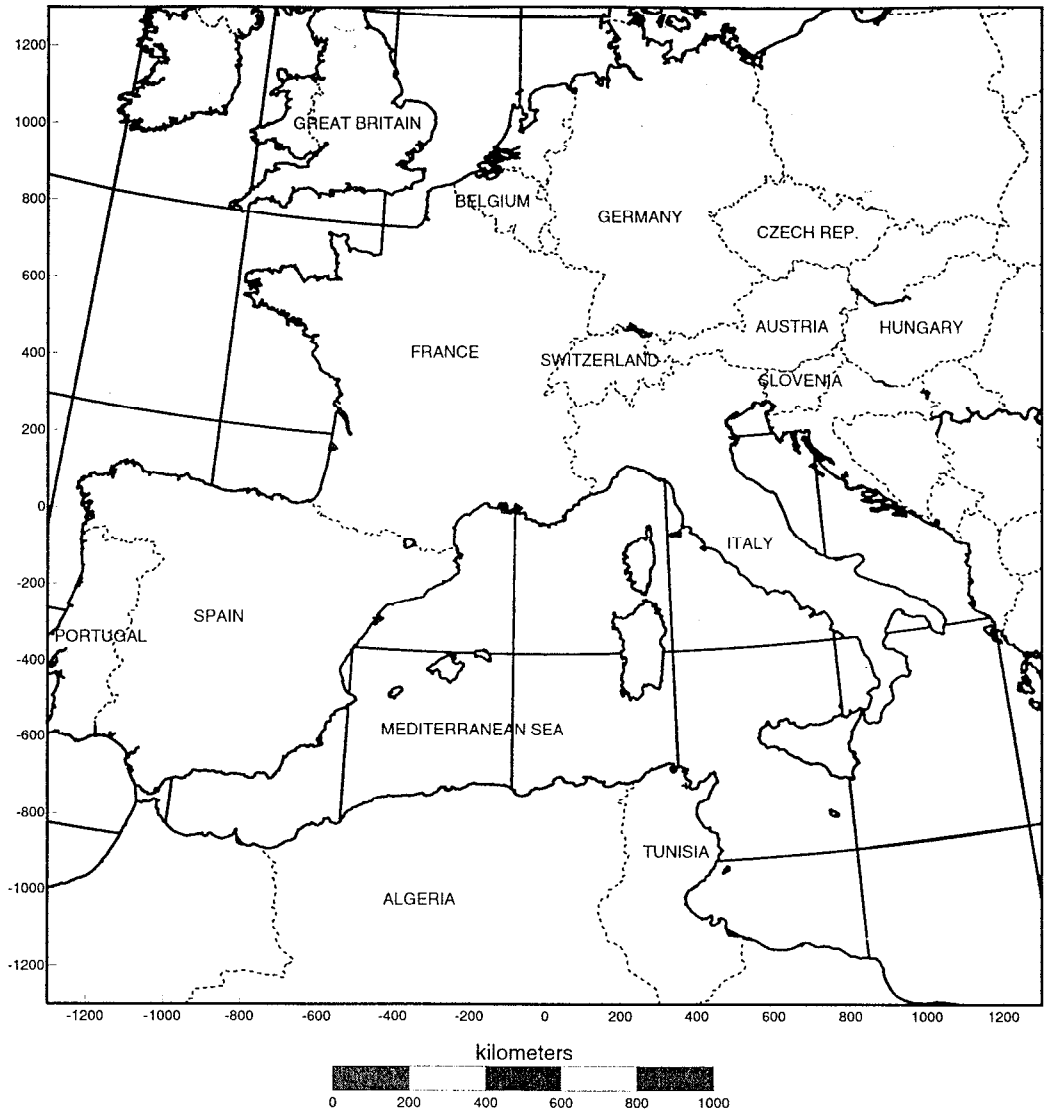

Figure 13. 2600 km model domain used for Sets 2 and 3.

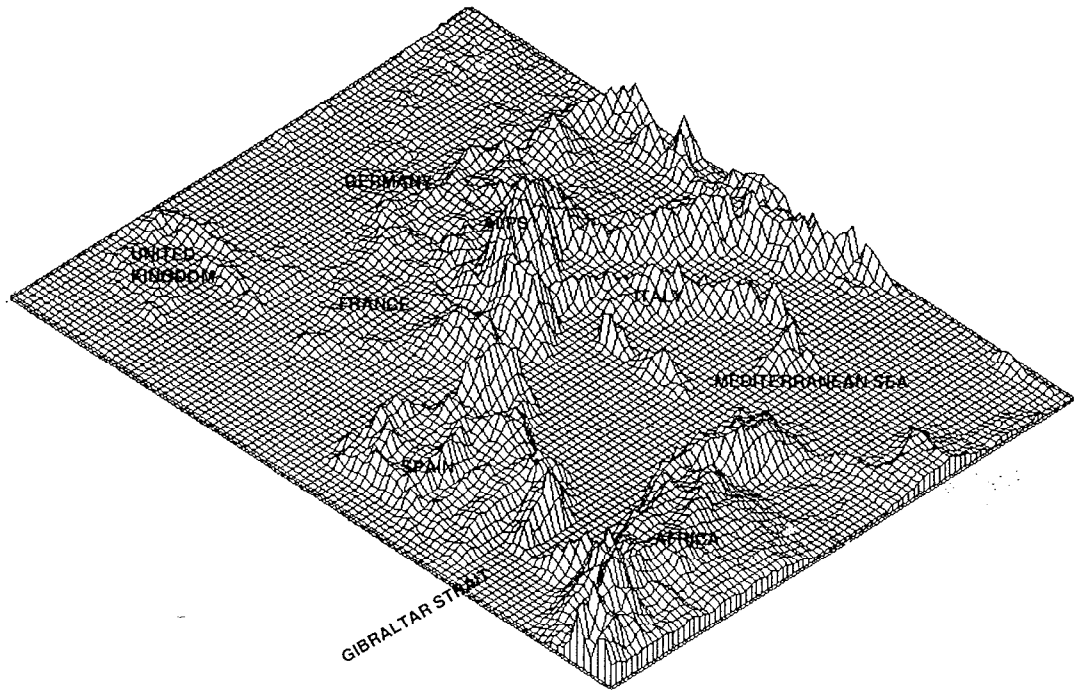

Figure 14. Perspective view of 2600 km terrain.

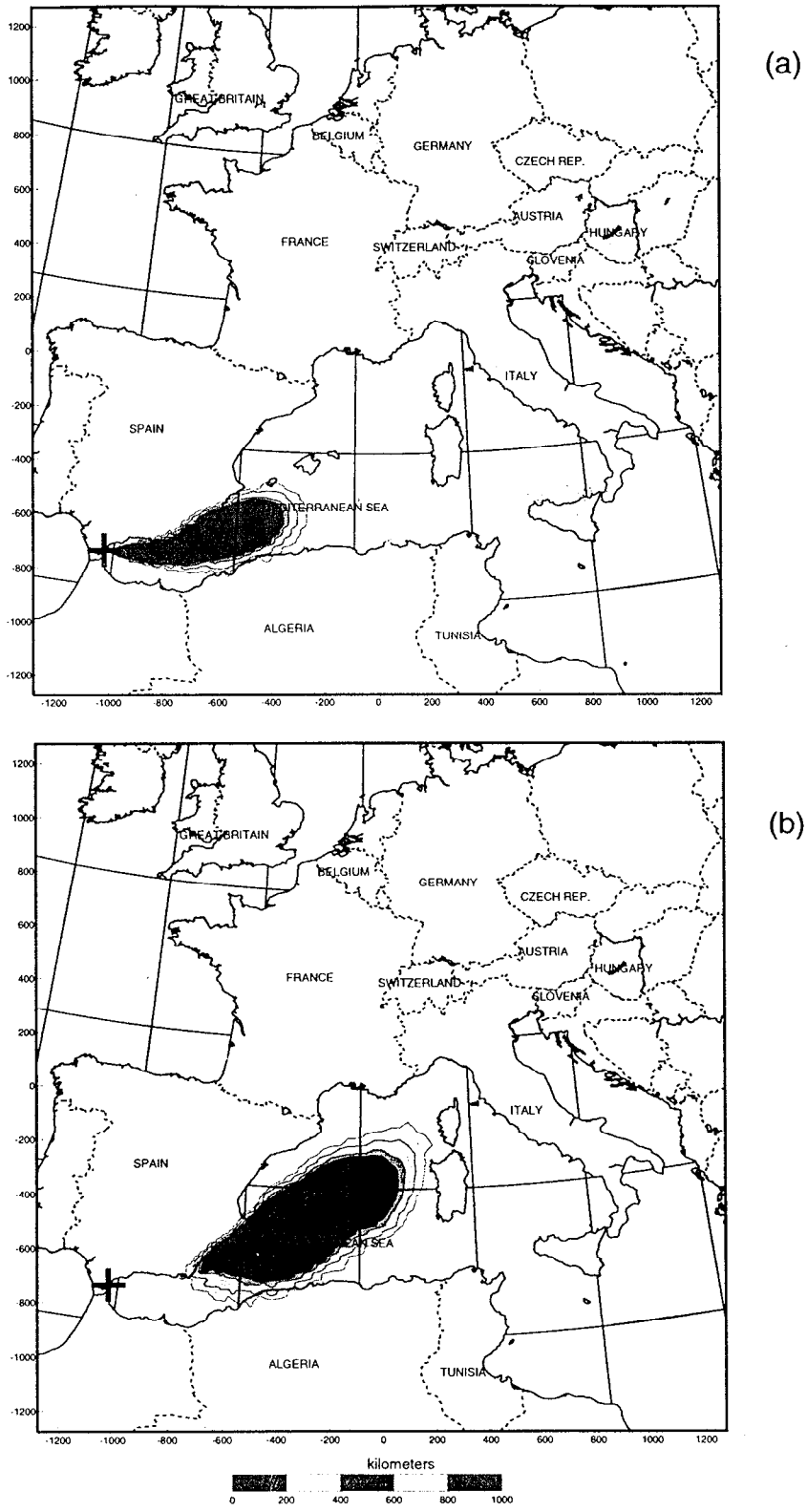

Figure 15. One-day average air concentration plots for Set 2 ending at 1500 UTC on (a) 30 May and, (b) 31 May 1998. Contours: >10 (outermost or lightest), >100, >500, and >1000 uBq/m3 (innermost or darkest).

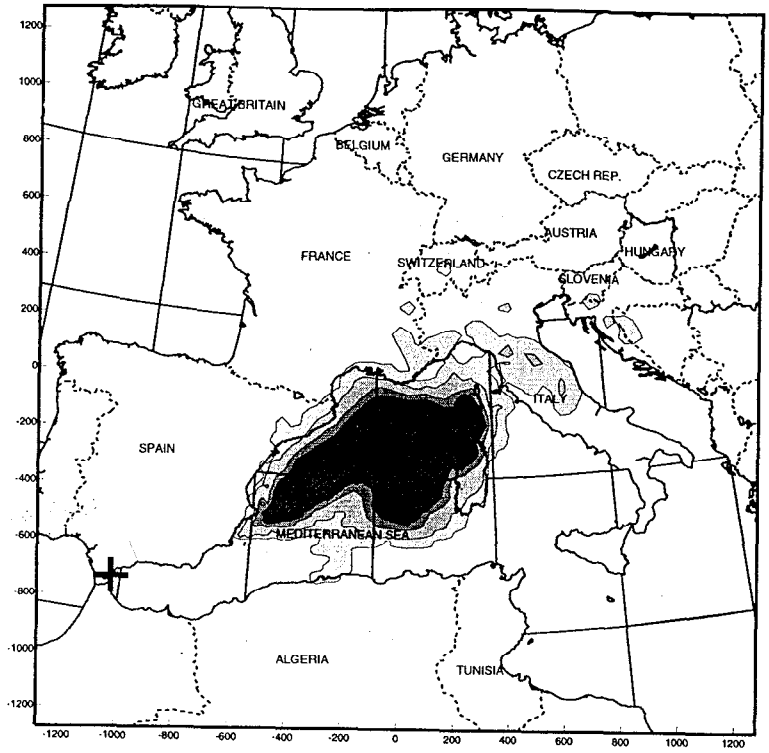

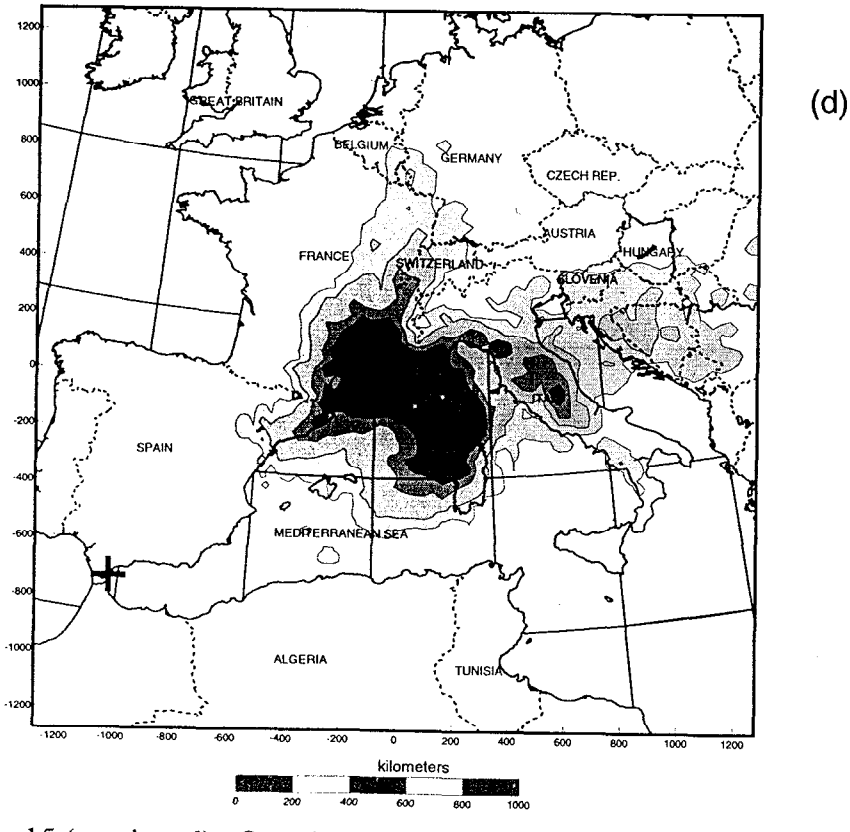

Figure 15 (continued). One-day average air concentration plots for Set 2 ending at 1500 UTC on (c) 1 June and, (d) 2 June 1998. Contours: >10 (outermost or lightest), >100, >500, and >1000 uBq/m3 (innermost or darkest).

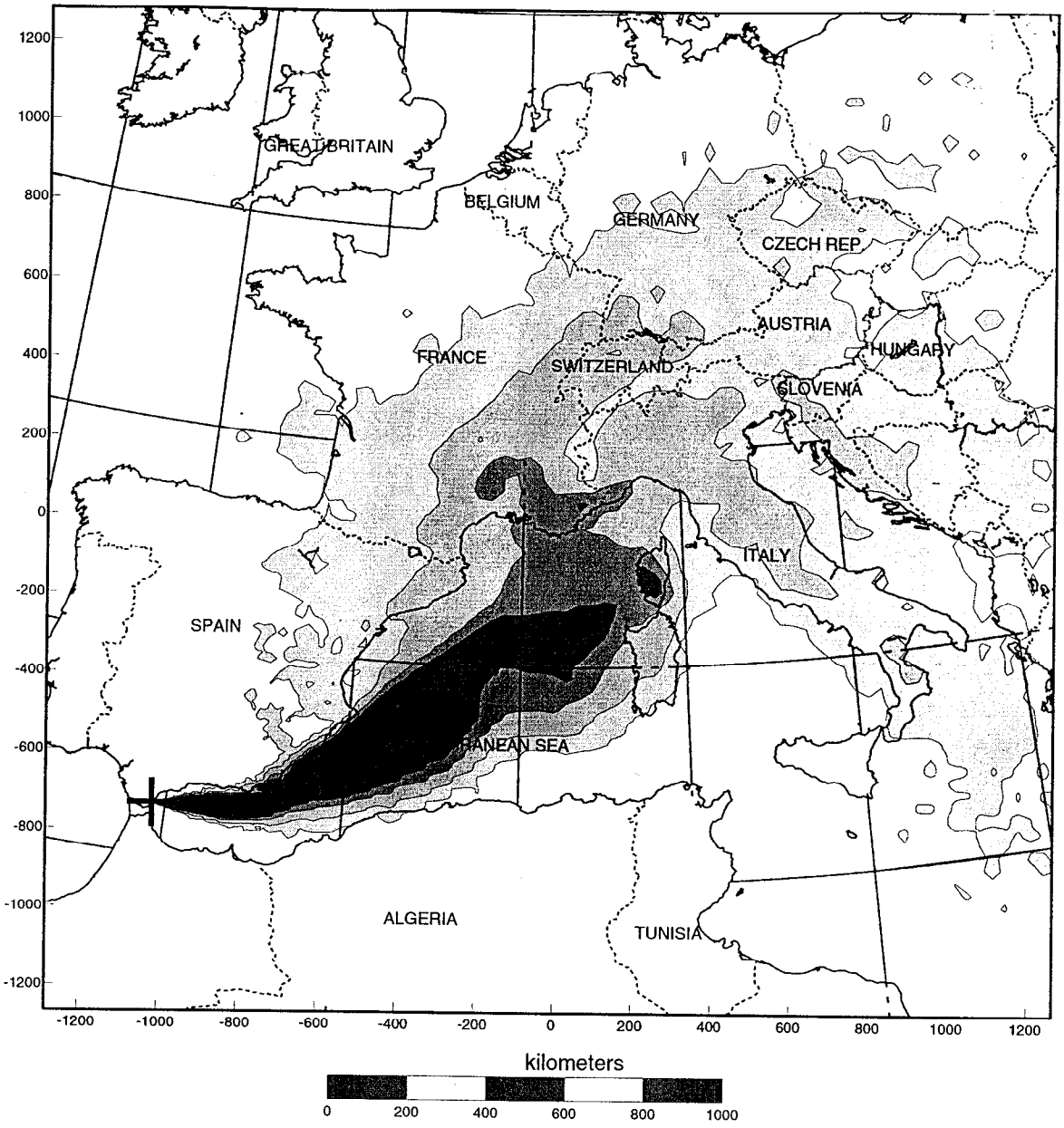

Figure 16. Seven-day average air concentration for Set 2 ending at 1500 UTC on 5 June 1998. Contours: >10 (outermost or lightest), >100, >500, and >1000 uBq/m3 (innermost or darkest).

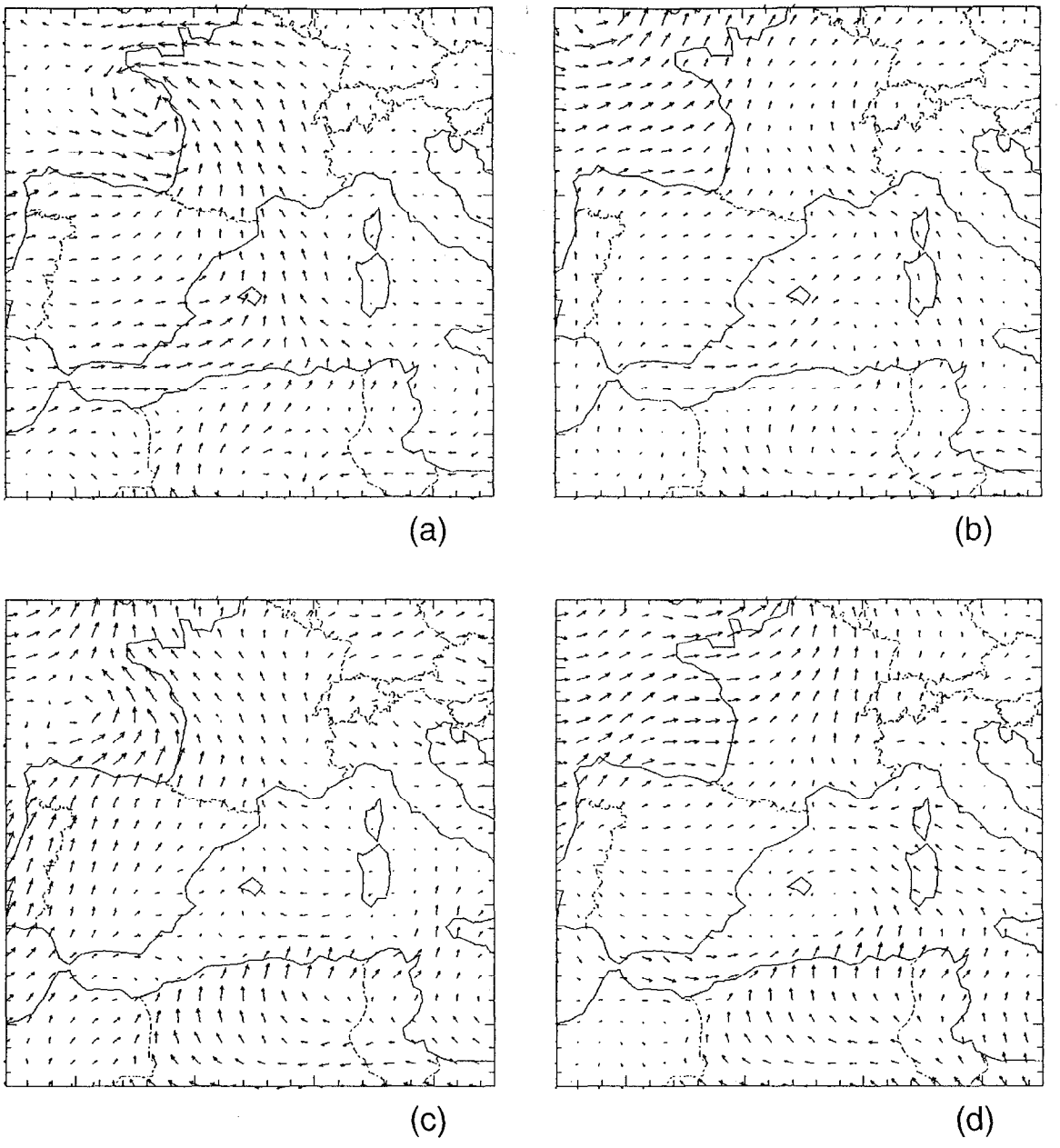

Figure 17. Set 3 near-surface model wind vectors at 0130 UTC for (a) 30 May, (b) 31 May, (c) 1 June, and (d) 2 June 1998.

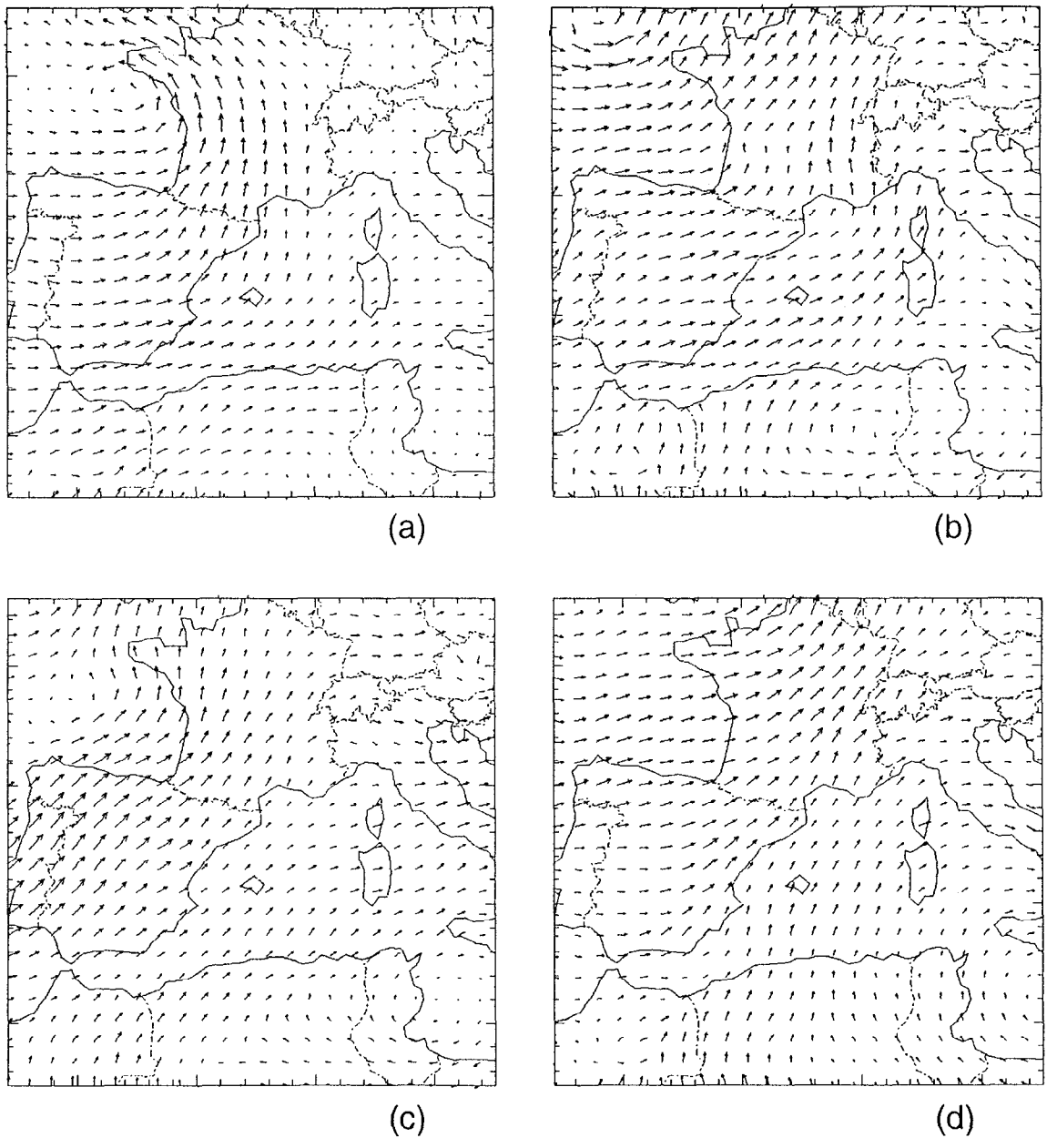

Figure 18. Set 3 model wind vectors at 1500 m above ground at 0130 UTC for (a) 30 May, (b) 31 May, (c) 1 June, and (d) 2 June 1998.

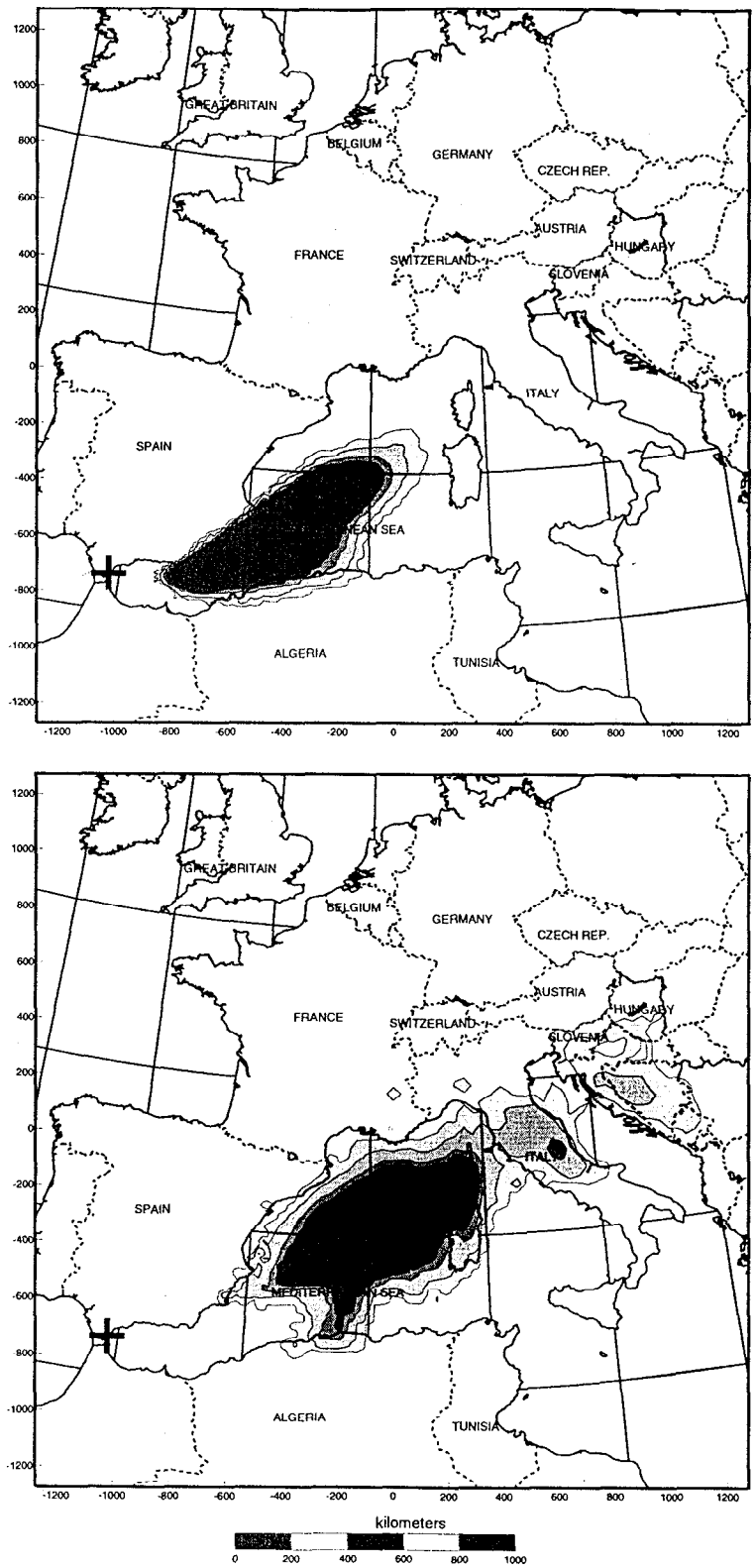

Figure 19. One-day average air concentration plots for Set 3 ending at 1200 UTC on (a) 31 May and, (b) 1 June 1998. Contours: >10 (outermost or lightest), >100, >500, and >1000 uBq/m3 (innermost or darkest).

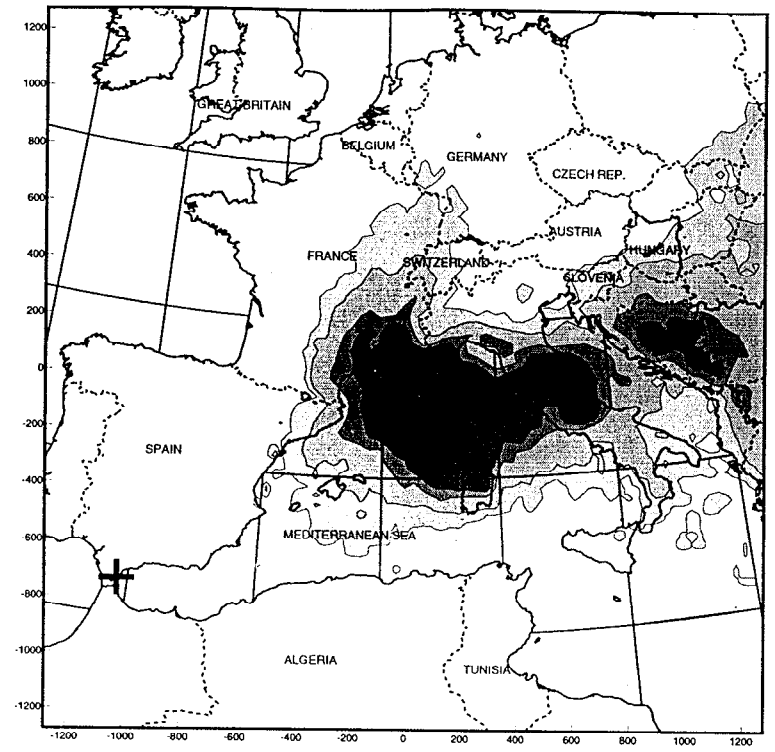

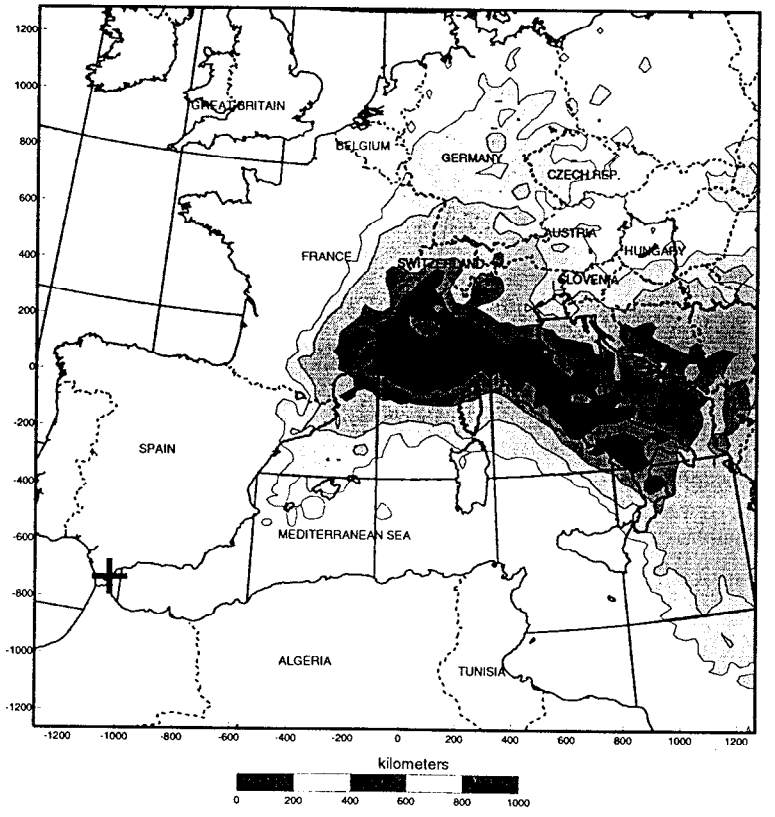

Figure 19 (continued). One-day average air concentration plots for Set 3 ending at 1200 UTC on (c) 2 June and, (d) 3 June 1998. Contours: >10 (outermost or lightest), >100, >500, and >1000 uBq/m3 (innermost or darkest).

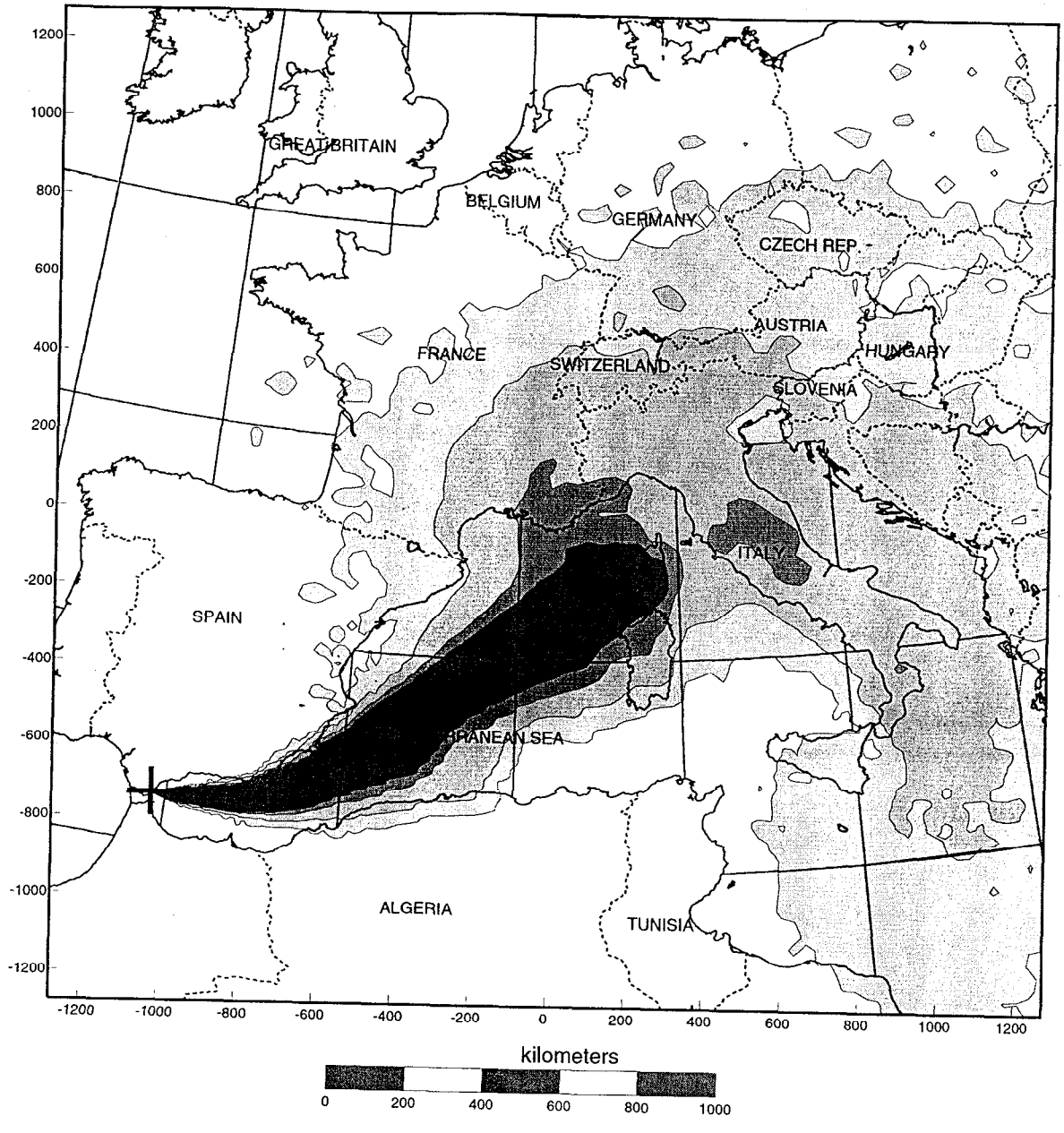

Figure 20: Seven-day average air concentration for Set 3 ending at 1200 UTC on 5 June 1998. Contours: >10 (outermost or lightest), >100, >500, and >1000 uBq/m3 (innermost or darkest).

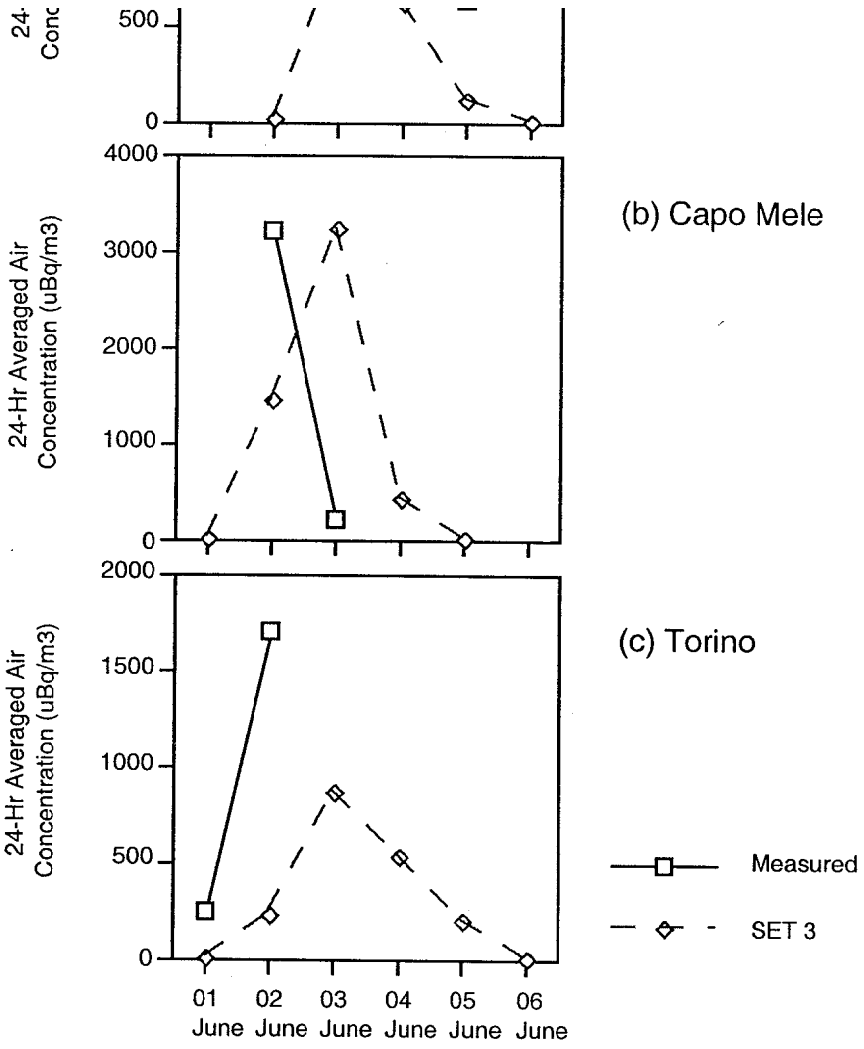

Figure 21. Comparison of Set 3 computed with measured daily average air concentrations for 1-6 June at (a) Vercelli, (b) Capo Mele, and (c) Torino, Italy.

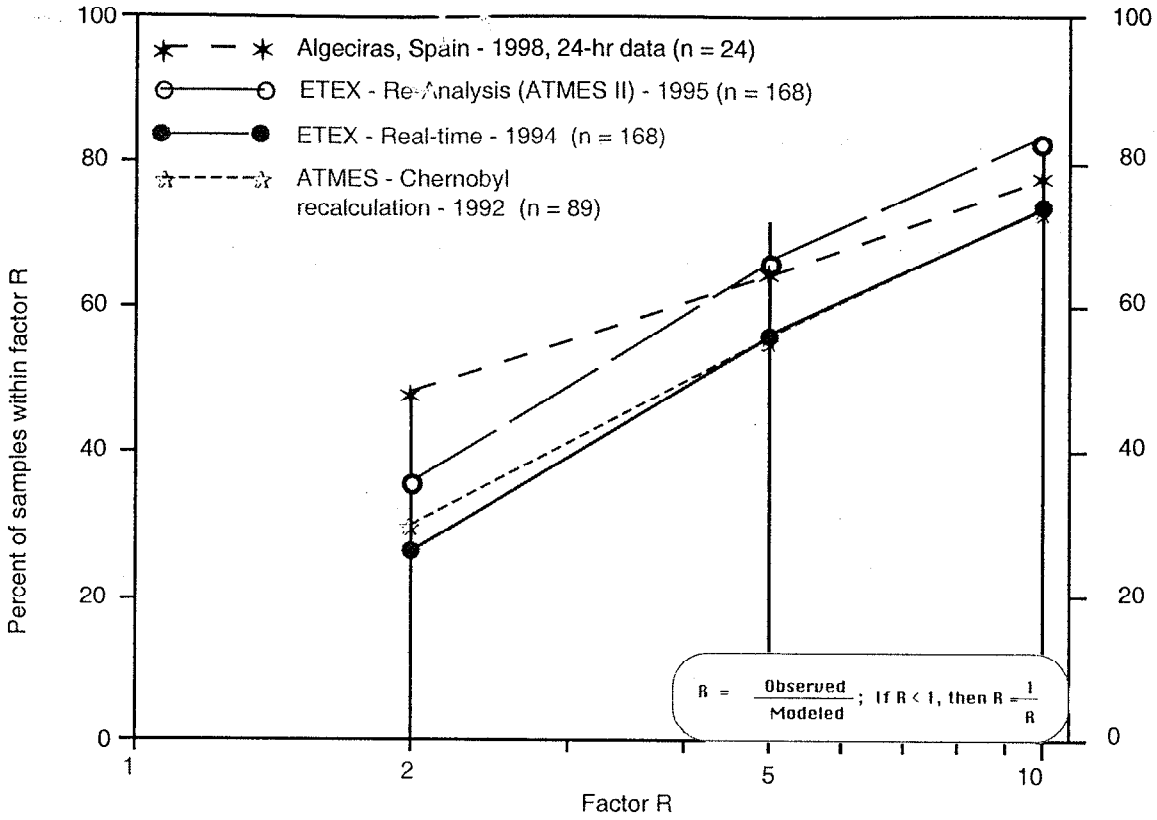

Figure 22. Algerciras model accuracy statistics compared with other ARAC continental scale model evaluation studies.

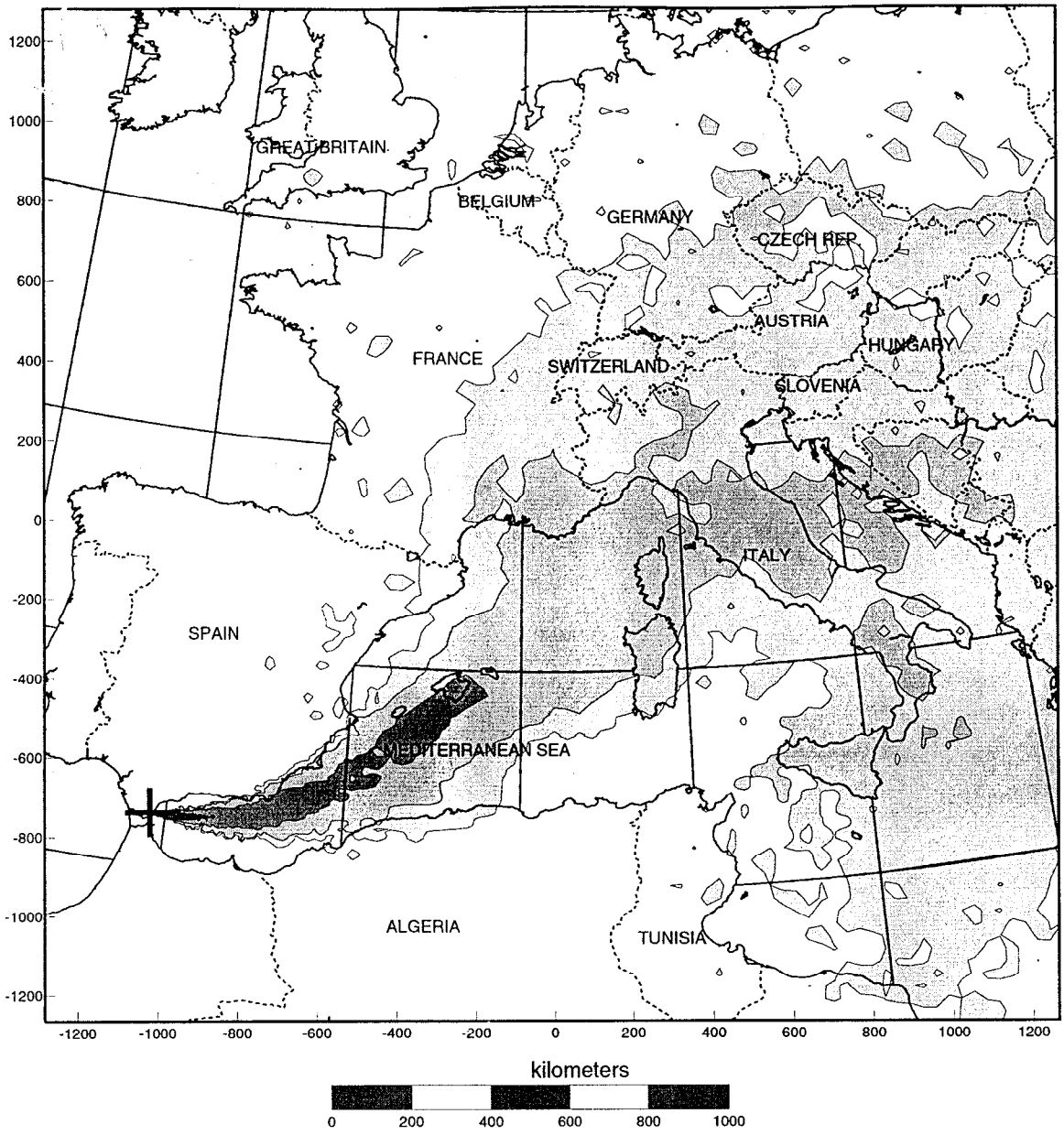

Figure 23. Effective Dose Equivalent from exposure to deposited material. Integrated ground shine dose from start of release through 1200 UTC on 18 June 1998. Contours: >1.0E-8(innermost or darkest), >1.0E-9, >1.0E-10, and >1.0E-11 Rem (outermost or lightest). Ground shine dose for water areas is irrelevantexcept for material deposited on ships at sea and not removed by rain or deck wash.